FEBRUARY 2017 | VOL. 27, NO. 2

Double Science Issue!

# GSA TODAY

A PUBLICATION OF THE GEOLOGICAL SOCIETY OF AMERICA®

## Impact of Seismic Image Quality on Fault Interpretation Uncertainty

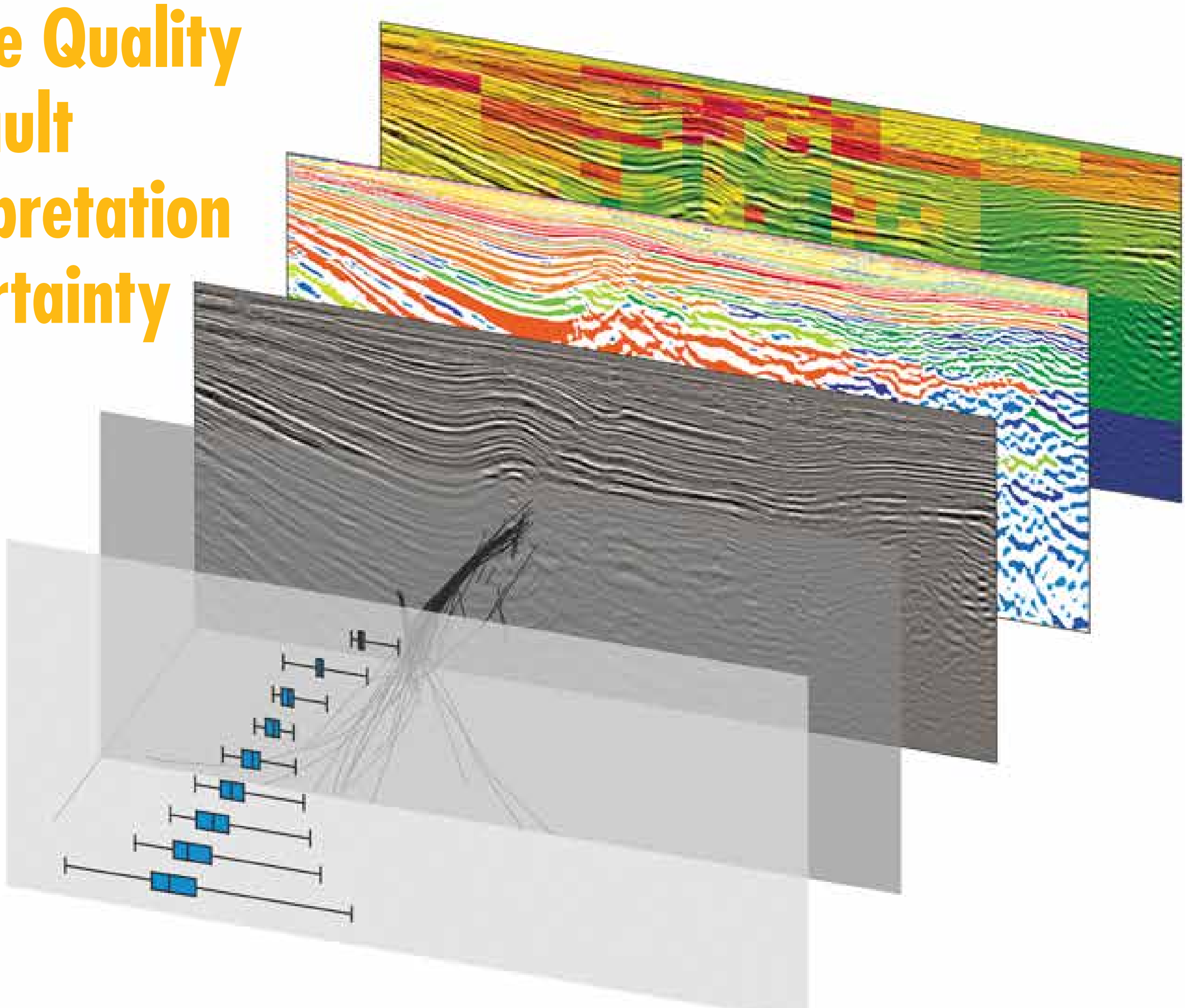

FEBRUARY 2017 | VOLUME 27, NUMBER 2

GSA TODAY

**GSA TODAY** (ISSN 1052-5173 USPS 0456-530) prints news and information for more than 26,000 GSA member readers and subscribing libraries, with 11 monthly issues (March/April is a combined issue). *GSA TODAY* is published by The Geological Society of America® Inc. (GSA) with offices at 3300 Penrose Place, Boulder, Colorado, USA, and a mailing address of P.O. Box 9140, Boulder, CO 80301-9140, USA. GSA provides this and other forums for the presentation of diverse opinions and positions by scientists worldwide, regardless of race, citizenship, gender, sexual orientation, religion, or political viewpoint. Opinions presented in this publication do not reflect official positions of the Society.



**Subscriptions: GSA members:** Contact GSA Sales & Service, +1-888-443-4472; +1-303-357-1000 option 3; gsaservice@geosociety.org for information and/or to place a claim for non-receipt or damaged copies. **Nonmembers and institutions:** *GSA TODAY* is US$97/yr; to subscribe, or for claims for non-receipt and damaged copies, contact gsaservice@geosociety.org. Claims are honored for one year; please allow sufficient delivery time for overseas copies. Periodicals postage paid at Boulder, Colorado, USA, and at additional mailing offices. Postmaster: Send address changes to GSA Sales & Service, P.O. Box 9140, Boulder, CO 80301-9140.

***GSA TODAY* STAFF**

**Executive Director and Publisher:** Vicki S. McConnell

**Science Editors: Steven Whitmeyer,** James Madison University Dept. of Geology & Environmental Science, 800 S. Main Street, MSC 6903, Harrisonburg, VA 22807, USA, whitmesj@jmu.edu; **Gerald Dickens,** Rice University School of Earth Science, MS-126, 6100 Main Street, Houston, Texas 77005, USA, jerry@rice.edu.

**Member Communications Manager:** Matt Hudson, mhudson@geosociety.org

**Managing Editor:** Kristen "Kea" Giles, kgiles@geosociety.org, gsatoday@geosociety.org

**Graphics Production:** Margo McGrew, mmcgrew@geosociety.org

**Advertising (classifieds & display):** Ann Crawford, +1-800-472-1988 ext. 1053; +1-303-357-1053; Fax: +1-303-357-1070; advertising@geosociety.org; acrawford@geosociety.org

**GSA Online:** www.geosociety.org
**GSA TODAY:** www.geosociety.org/gsatoday

Printed in the USA using pure soy inks.

THE GEOLOGICAL SOCIETY OF AMERICA®



# Double Science Issue!



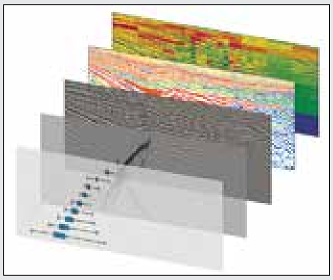

**Cover:** Where lies the fault? See related article, p. 4–10.



***Inside* Cover:** Chakpaktas: Paleosols and terrestrial sediments exposed on the north shore of Lake Zaysan. Lake Zaysan to the left. Photo credit: Daniel E. Ibarra. See related article, p. 19–26.



## New Comment & Reply Posted Online

www.geosociety.org/gsatoday/comment-reply/

**COMMENT:**
**Finney & Edwards Article**
Jan Zalasiewicz and 25 others, doi: 10.1130/GSATG309C.1.

**REPLY:**
**Zalasiewicz et al. Comment**
Stanley C. Finney and Lucy E. Edwards, doi: 10.1130/GSATG326Y.1

**ORIGINAL ARTICLE:**
**The "Anthropocene" epoch: Scientific decision or political statement?**
*GSA Today*, v. 26, no. 2, p. 4–10, doi: 10.1130/GSATG270A.1.

# Impact of seismic image quality on fault interpretation uncertainty

***Juan Alcalde,*** *Geology and Petroleum Geology, University of Aberdeen, School of Geosciences, Kings College, Aberdeen, AB24 3UE, UK, and School of GeoSciences, University of Edinburgh, West Mains Road, Edinburgh, EH9 3FE, UK, juan.alcalde@abdn.ac.uk;* ***Clare E. Bond,*** *Geology and Petroleum Geology, University of Aberdeen, School of Geosciences, Kings College, Aberdeen, AB24 3UE, UK, clare.bond@abdn.ac.uk;* ***Gareth Johnson,*** *School of GeoSciences, University of Edinburgh, West Mains Road, Edinburgh, EH9 3FE, UK, g.johnson@ed.ac.uk;* ***Jennifer F. Ellis*,*** *Midland Valley Exploration Ltd, 2 West Regent Street, Glasgow, G2 1RW, UK, ellisj11@cardiff.ac.uk; and* ***Robert W.H. Butler,*** *Geology and Petroleum Geology, University of Aberdeen, School of Geosciences, Kings College, Aberdeen, AB24 3UE, UK, rob.butler@abdn.ac.uk*

## ABSTRACT

Uncertainty in the geological interpretation of a seismic image is affected by image quality. Using quantitative image analysis techniques, we have mapped differences in image contrast and reflection continuity for two different representations of the same grayscale seismic image, one in two-way-time (TWT) and one in depth. The contrast and reflection continuity of the depth image is lower than that of the TWT image. We compare the results of 196 interpretations of a single fault with the quality of the seismic image. Low contrast and continuity areas correspond to a greater range of interpreted fault geometries, resulting in a broader spread of fault interpretations in the depth image. Subtle differences in interpreted fault geometries introduce changes in fault characteristics (e.g., throw, heave) that are critical for understanding crustal and lithospheric processes. Seismic image quality impacts interpretation certainty, as evidenced by the increased range in fault interpretations. Quantitative assessments of image quality could inform: (1) whether model-based interpretation (e.g., fault geometry prediction at depth) is more robust than a subjective interpretation; and (2) uncertainty assessments of fault interpretations used to predict tectonic processes such as crustal extension.

## INTRODUCTION

Interpreting seismic reflection data is the principal approach for obtaining a detailed understanding of the geological structure of the subsurface. Central to these endeavors is the ability to trace faults. The resulting interpretations of fault patterns are used to infer a wide variety of tectonic properties—for example: estimations of upper crustal stretching during lithospheric extension (e.g., Kusznir and Karner 2007); kinematic connectivity and stretching directions (e.g., Baudon and Cartwright, 2008); and polyphase reactivation and inversion (e.g., Underhill and Paterson, 1998; Badley and Backshall, 1989). Fault interpretations are important components in the prediction of hydrocarbon reservoir volumes in structural traps, and in forecasting the integrity and performance for structurally complex reservoirs (e.g., Richards et al., 2015; Yielding, 2015; Wood et al., 2015; Freeman et al., 2015). However, in publications, faults are commonly shown as single, deterministic interpretations—even though there are uncertainties in these seismic interpretations that will impact the application of the interpretation. A single seismic image can comprise a range of interpretations with intrinsic probabilities (Bond et al., 2007; Hardy, 2015). Despite the importance of fault interpretations, remarkably few publications or indeed training materials explain how faults are interpreted on seismic reflection profiles or discuss the uncertainties in the interpretations. Here we explore how image quality impacts fault interpretation, using outputs from an interpretation exercise.

Faults may be characterized as quasi-planar features that offset geological markers. It is rare that the fault surfaces themselves generate seismic reflections. Therefore, on seismic images, fault geometries are established chiefly by linking the terminations of stratal reflectors (e.g., Bahorich and Farmer, 1995). However, there are many other explanations for reflector termination, some geophysical (e.g., noise, processing effects, anomalous changes in velocity) and some geological (e.g., depositional facies changes, channels, unconformities), that are not always easy to distinguish, so there are ambiguities in fault interpretation. Subtle differences in fault interpretation introduce changes in the geometric characteristics of the faults (e.g., throw, heave), with, for example, impact on the determination of stretching factors for sedimentary basins. For basins in a late stage of being explored, 3D seismic data are often employed because they generally provide a higher spatial resolution and geometric continuity compared with even closely spaced grids of 2D seismic profiles (Cartwright and Huuse, 2005; Gao, 2009), but there can still be significant uncertainty in structural interpretation. Regardless of the development of 3D seismic methods, 2D data continue to underpin regional tectonic studies and frontier basin exploration (e.g., Platt and Philip, 1995; Thomson and Underhill, 1999; Gabrielsen et al., 2013). Much of the understanding of fault geometry is based on heritage 2D data from the 1980s (e.g., Freeman et al., 1990), even if enhanced by subsequent 3D studies (e.g., Cartwright and Huuse, 2005). Furthermore, training materials in fault interpretation (e.g., Shaw et al., 2005), as well as knowledge-sharing resources (i.e., books and articles), are chiefly two-dimensional, presented in paper or on computer screen. In summary, 2D interpretation is a fundamental and important part of most seismic interpretations irrespective of whether the

*GSA Today*, v. 27, no. 2, doi: 10.1130/GSATG282A.1

*Current address: Cardiff University School of Earth and Ocean Sciences, Main Building, Park Place, Cardiff, CF10 3AT, UK.

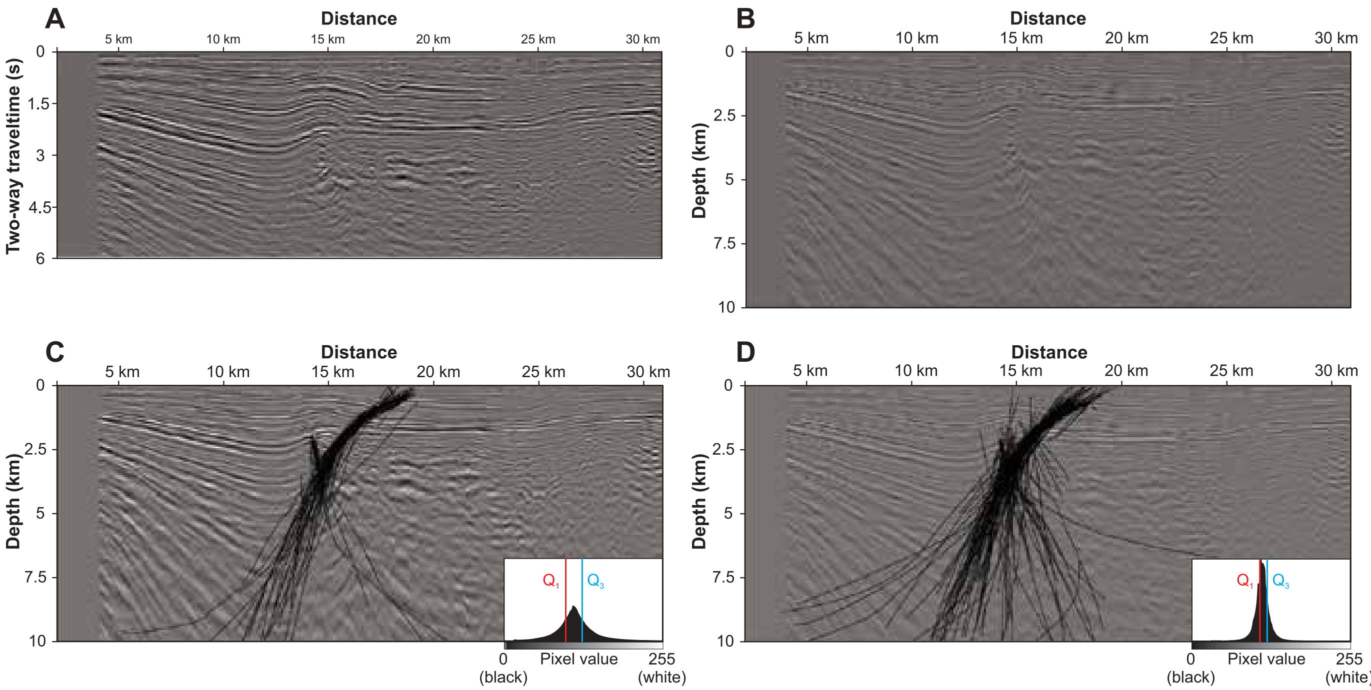


**Figure 1. Seismic sections used in the interpretation experiment. (A) Seismic section in two-way travel time (TWT). (B) Seismic section in depth. (C) and (D) stacked results of the interpreted faults in TWT and depth (respectively). The figure includes the histogram of the corresponding section. In the histograms, the *x*-axis represents the possible gray values (from 0-black to 255-white) and the *y*-axis the number of pixels found for each value. Note that the sections conserve the vertical scale in which they were presented to the participants and that the results in TWT were converted to depth, to be comparable with those interpreted in the depth section. The sections are courtesy of BP/GRUPCO. $Q_1$ and $Q_3$—first and third quartiles.**

data are available as 2D lines or 3D volumes. In spite of its importance, the impression given by these training materials and by the expert community is that fault interpretation in seismic imagery is routine and carries little uncertainty.

## HOW DO WE SEE SEISMIC IMAGES?

Seismic data are viewed and interpreted manually as images. There are a number of visual factors that affect how we perceive objects, including color, intensity, hue, and perspective (e.g., Froner et al., 2013). These factors determine the saliency of the different elements that form an image. Visual saliency refers to the distinctiveness of an element; i.e., the capacity to draw the attention of the viewer (e.g., Kadir and Brady, 2001; Kim et al., 2010), and is mainly dependent on its distinction from nearby elements (Cheng et al., 2011). Visual saliency produces biases in favor of the most prominent elements (Reynolds and Desimone, 2003), and hence influences interpretation. As such, increasing image contrast enhances differences between prominent elements in an image (Reynolds and Desimone, 2003).

Classically, seismic imagery is presented as a grayscale, although it is now commonly visualized in color, using either linear or nonlinear color spectrums (Froner et al., 2013). Nonlinear color spectrums are often used to highlight maximum and minimum amplitude reflectors. When employing an 8-bit black-and-white computer render, image contrast represents the range in amplitude of seismic reflection data as 256 pixels in different shades of gray. Similarly, reflection continuity (the saliency of a reflector) is represented by adjoining pixels of the same, or a similar, shade of gray. Modern 64-bit computers can display images in millions of gray or color shades. However, human perception of images presented in gray scale is poorly understood and an active area of research (Song et al., 2010; Radonjić et al., 2011). Our aim is to test if even "simple" 8-bit grayscale visualizations of seismic images of different quality have an impact on interpretation outcome.

## INTERPRETATION EXPERIMENT

We presented a seismic image to 196 interpreters in a controlled experiment and compared their interpretations of a major fault in the seismic image with the image quality. The seismic reflection image from the Gulf of Suez (Fig. 1) was presented either in two-way travel time (TWT, Fig. 1A)—70 subjects, 36% of the interpretations—or in depth domain (Fig. 1B)—126 subjects, 64% of the interpretations (Figs. 1C and 1D, respectively). The participants were asked to "interpret the major fault crossing the section and the main sedimentary horizons as deep as they could." They were also asked to provide further annotation and/or sketching to support their interpretations. In this contribution, we focus purely on the fault interpretations as drawn by the participants on the seismic image. Participants had up to 30 minutes to complete their interpretations. The interpreters' proficiencies were highly diverse, and their experience ranged from unexperienced students to interpretation specialists with more than 30 years of experience.

The seismic section used in the experiment was 31 km long and extended to 6 s TWT (Fig. 1A). The seismic image included a lateral disruption of the reflections in the central part, generally interpreted as a fault, but with some degree of uncertainty as to the fault's placement, geometry, and extent. The TWT section was converted to depth using a simple velocity model in Move™, described by Equation (1):

$$Z = V_0 \frac{(e^{kt} - 1)}{k} \quad (1)$$

where $Z$ is the depth in meters, $V_0$ is the initial velocity (1500 $ms^{-1}$), $t$ is one-way travel time, and $k$ is the rate of change in velocity with increasing depth (0.5). The depth conversion located the bottom of the section at 10.5 km depth. The depth conversion was completed on a bitmap of the seismic reflection image, which linearly stretches the image. The result is a depth section with apparently lower reflectivity and contrast than the original TWT image and 18% longer, due to this stretching. With the exception of depth conversion, both the TWT and depth images share identical processing workflows. The actual depth conversion method used is not important for our experiment; it is the difference in image quality the process creates that concerns us.

## IMAGE ANALYSIS

The image analysis undertaken focused on the pixel intensity contrast and reflection continuity (referred to hereafter as "contrast" and "continuity," respectively) of the TWT and depth sections (see Fig. S1 in GSA's Supplemental Data Repository[1]). For the image analysis, each seismic image was subdivided into cells of 7.2 km (length) × 1 km (depth) (1135 × 450 pixels). The area encompassing the participants' fault interpretations was subdivided into smaller cells, 1.6 km × 0.4 km (216 × 163 pixels), in order to provide detailed image analysis information in the area of interest. For ease of comparison of our results, the seismic images are both shown with a vertical scale in depth in all figures (except Fig. 1A).

To analyze the image contrast we extracted grayscale distributions for the pixels in each cell for the two uninterpreted images. The distributions range from pixel number 0 (black) to 255 (white): the wider these distributions are (i.e., the more pixel values close to the extremes of 0 and 255), the more contrast the image has; the narrower the pixel distribution, the more similar the pixel values are and thus the lower the contrast. The first and third quartiles ($Q_1$ and $Q_3$) from these distributions were subtracted in order to calculate the interquartile range ($I_Q$) of the distributions. We use the interquartile range as an analogue for visual contrast: the wider the $I_Q$ of the cell, the higher the contrast and vice versa. Each cell in the images is colored according to its $I_Q$ value in order to display graphically the contrast analysis results.

To analyze the reflector continuity, the images were first converted into a binary, i.e., a black and white image. This was performed using ImageJ software (Schneider et al., 2012) by setting an automatic threshold level based on the histograms of the two images. This threshold divides the pixel histogram in two halves, assigning black or white color to all the pixels. As a result, the seismic wave reflections are separated into isolated black bodies, corresponding to the positive amplitude reflections in this particular case, included in a white background. A macro for the software ImageJ (Heilbronner and Barrett, 2013) was used to measure and analyze these resultant bodies. In the analysis, the length of the major axis of each reflection is calculated, using a best-fit ellipse method, and each reflection is then colored based on this length value using a color scale.

## INTERPRETATION OUTCOMES

Interpretations of the major discontinuity of reflectors (faults) located in the middle of the seismic images and related splay faults (327 elements in total) were used in the analysis. Of these elements, 116 correspond to the interpretations of the TWT image (Fig. 1C) and 211 to the interpretations of the depth seismic image (Fig. 1D). In general, variability in fault placement position (the spread in fault interpretations) increases with depth, and this observation is more pronounced in those interpretations derived from the depth image. The difference in fault placement spread between the two images is at a maximum at 5 km depth. Below this point, the amount of interpreted faults dipping to the right is greater in the depth section (23 faults) than in the TWT section (5 faults). The effect of the difference in the populations of TWT and depth interpretations was analyzed by randomly selecting 70 of the depth interpretations for comparison with the TWT interpretation population of 70. Because these were found to be similar to the full-depth interpretation analysis, we conclude that the population size had no effect on the results.

Quantification of the variability in fault placement for the interpretation populations were computed at nine depth markers in each seismic image (Fig. 2). The four quartile and outlier positions for the fault interpretation populations were calculated at each depth marker (results of the analysis are shown in Fig. 2, overlying the image analyses). The interquartile fault range (the distance between the first and third quartiles) provides a good estimation of the fault placement spread within each of the interpretation populations at a given depth (continuous black lines in Fig. 2, created from joining the quartiles between depth markers). We use the interquartile range of fault placement within each fault interpretation population as an indicator of fault placement uncertainty for each seismic image. The interquartiles show that fault spread remains similar in the upper 3.5 km. From 3.5 km downward, the interquartile fault range in the depth image increases until, at the base of the seismic image, the interquartile width is twice that observed in the TWT image. The increase in fault spread defined by the interquartile trend linearly increases in the TWT image with depth. In the depth image, the first quartile follows a similar path to that of the TWT image, but the third quartile is more heterogeneous (wavy) and is offset to the right with respect to the third quartile line in the TWT image. Meanwhile, the outliers (dashed black lines in Fig. 2) show a similar general pattern with fault spread increasing with depth, but with a greater variability and heterogeneity. The fault placement outliers for the fault interpretations of the TWT image show a convergent trend down to 2 km in width at ~4 km depth before the fault placement spread increases to ~15 km at the base of the image. The fault placement outliers from the depth interpretation show a relatively constant spread (~4.5 km width) down to 3 km depth. Below this point, fault spread

[1] GSA Supplemental Data Repository Item 2017031, image analysis methods, is online at http://www.geosociety.org/datarepository/2017/. If you have questions, please email gsatoday@geosociety.org.

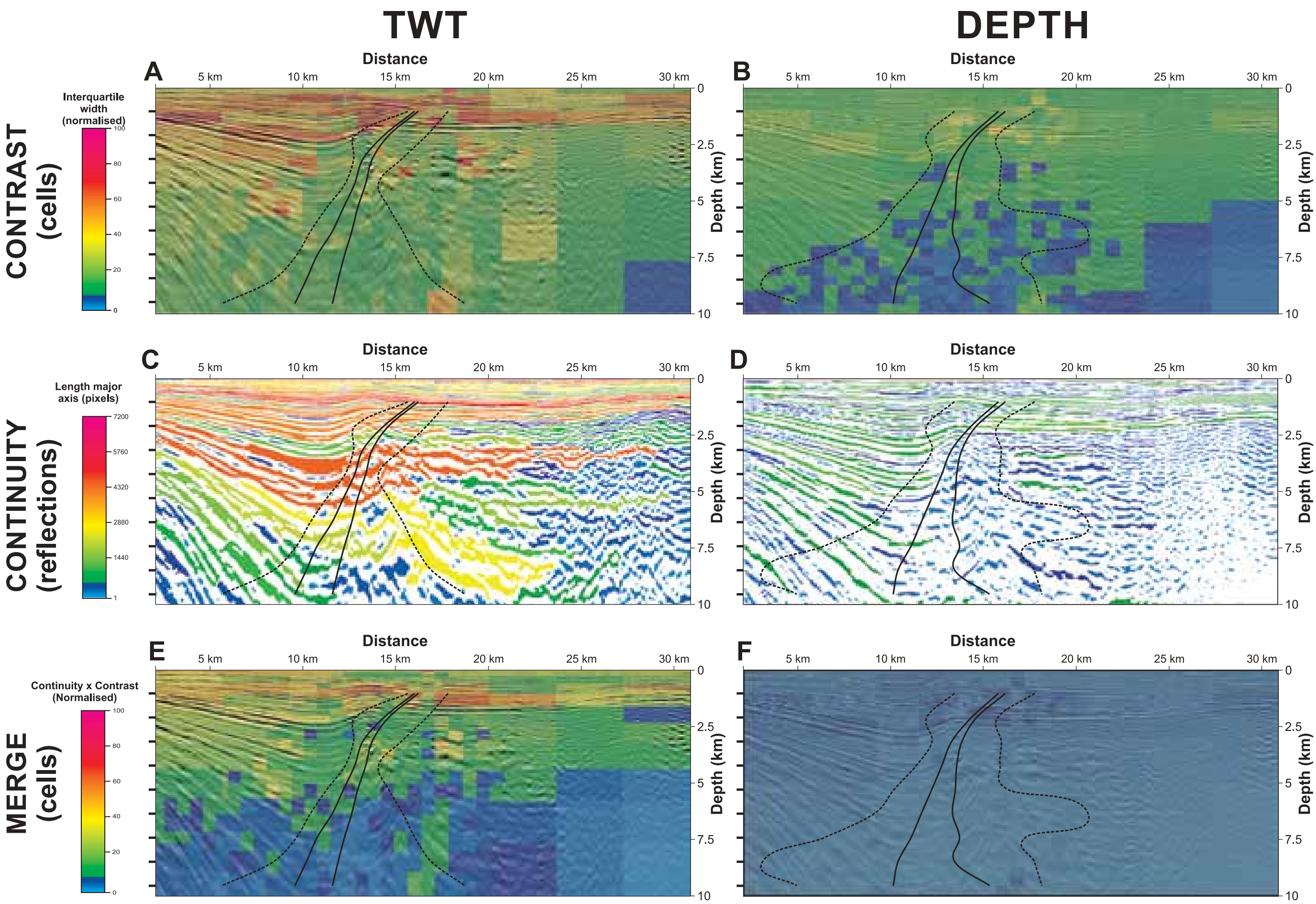


**Figure 2. Results of the analysis carried out in two-way travel time (TWT) (A, C, and E) and depth (B, D, and F) seismic sections with the respective fault spread superimposed (outlier limits marked with dashed lines; quartiles 1 and 2 marked in continuous lines). (A) and (B) contrast analysis—warm colors represent high values in interquartile difference (i.e., high contrast) and cold colors represent low values (i.e., low contrast). (C) and (D) continuity analysis—reflections colored according to the length of their major axis, with warm colors indicating long lengths (i.e., high continuity) and cold colors short length (i.e., low continuity). (E) and (F) merge of the two analyses—the results have been combined in a 1:1 relation; that is, the contrast and continuity values have been multiplied and normalized to 100. Note that the TWT results have been depth-converted for comparison (i.e., located at the same point) to the depth results. The black lines at the left side of the images mark the depths of the nine positions at which the fault placement for the interpretation populations was computed in each seismic image.**

increases with depth, resulting in a 15-km spread in fault interpretations at the base of the seismic image. There is also a clear difference in the length of the faults interpreted. The depth of the first and last point of the faults were measured, resulting in an average depth of 4.7 km and 6.6 km for the faults interpreted in TWT and depth, respectively.

## IMAGE QUALITY

### Image Contrast

Contrast in the TWT seismic image is almost three times greater than in the depth image (Figs. 1C and 1D). Detailed contrast analysis of both seismic images shows a decrease in contrast with depth as well as higher contrast to the left of the fault location as compared to the right (Figs. 2A and 2B). There is a visible spatial association between lower contrast areas in the seismic imagery and a larger spread in fault placement certainty (Figs. 2A and 2B). This effect is especially visible in areas with very low $I_Q$, which correspond to maximum fault placement dispersion (i.e., dark green and blue colors in Fig. 2B). In the TWT seismic image, the $I_Q$ values remain moderate when compared to the depth image. This may account for the smaller interquartile range in fault placement in the lower half of the TWT image in comparison to the depth image (Fig. 2B).

The outlier fault interpretations (dashed lines in Figs. 2A and 2B) are also likely to have been affected by image contrast; indications of this influence can be seen in Figure 2A, where the left outlier line follows the yellow/green pixel contrast binning boundary at 2.5–7 km depth. The convexity of the right outlier toward the third quartile at 3.5 km depth and ~15 km distance along the TWT seismic image was associated with the existence of higher contrast cells (yellow colors) in comparison to surrounding cells at this point (Fig. 2A).

### Reflection Continuity

Reflection continuity decreases with depth in the seismic images and to the right of the main fault. Reflection continuity is, on average, 63% smaller in the depth image than in the TWT image (Figs. 2C and 2D). We associate this dramatic reduction in continuity to the decrease in contrast as a result of the depth conversion. Interpreted faults tend to cross areas with lower reflection continuity. This is not surprising, because faults that cut and disrupt rock layers with the same reflective physical properties would create low reflection continuity. The fault interpretations coincide with where reflectors from the left join those coming from the right, at ~13–16 km along the seismic image, at ~6 km depth. The third quartile of the TWT interpretations follow this boundary. In the depth seismic image this joining of reflectors is less clear (potentially due to the lack of reflectivity/continuity), and the third quartile is more variable, especially in the deeper part below 5 km. The greater amount of faults dipping to the right below 5 km depth in the depth image can be explained by a lack of reflection continuity at distances along the section line >13 km, and 5 km depth (Fig. 2D). In the TWT image, right-dipping faults have to be interpreted crossing strong, continuous reflections below 5 km, and most right-dipping fault interpretations stop at shallower depths (from 17 fault interpretations at 3 km depth to only 5 at 5 km depth). In the depth image, the reflections are more discontinuous and fault interpretations continue to greater depths. The extent of the outliers also seems to be affected by reflection continuity. In the TWT seismic image for example, the right outlier line coincides with a break in reflection continuity between 4–10 km depth (Fig. 2C); in the depth image, the right outlier stays to the left of a package with more continuous horizontal reflections, located at 2.5–5.5 km depth (Fig. 2D).

### Combined Image Analysis

The analysis of contrast and continuity highlighted spatial associations between image quality and fault interpretation (Figs. 2A–2D). In reality, the image, as viewed by the interpreter, is the result of combining both contrast and continuity. In an attempt to merge the results of the contrast and continuity analyses, the continuity analysis was converted into a cell model, based on the contrast grid. This conversion assigned the maximum continuity value contained within a cell to each cell in the grid. To merge the analyses, cells in the new continuity cell model were multiplied with the values from the respective cells from the contrast analysis. In spite of the potential different impact of the two parameters on the interpreters and their relative co-dependency (i.e., enhancing the contrast can enhance the continuity), creating a combined parameter provides a general visualization of image quality. The results were normalized by representing the maximum value as 100 and the minimum as zero. The resulting merged models for the depth-converted TWT and depth images are shown in Figures 2E and 2F.

There is a diffuse horizontal boundary in the merged values in the TWT image at ~4.5 km depth (Fig. 2E), marking a change from “green” and hotter colors at shallower levels to lower “blue” values as depth increases. This 4.5 km depth marks the point at which the distance between the first and third quartiles increases from 523 m to more than double (1234 m) at the bottom of the section. This boundary also coincides with the average depth of the interpreted TWT faults, suggesting that it marks a clear increment in the uncertainty of the image for interpretation. Faults are interpreted until a deeper point in the depth image, potentially because this boundary in image quality is less perceptible. The positions of the outlier interpretations show a greater change, from a narrow converging spread to divergent with the spread increasing with depth. In the case of the depth image (Fig. 2F), this boundary is less noticeable, possibly due to the overall low values and poor image quality, although fault spread does increase with depth below 4.5 km. The results suggest that there may be a contrast and continuity threshold within the seismic images beyond which the fault interpretations are almost unconstrained by the data.

## IMPACT ON INTERPRETATION

The experiment outlined above shows that image contrast and the continuity of features both impact on the interpretation outcome of the seismic imagery. Interpreters are less prone to cross stratal reflections if they are “strong” (i.e., high contrast and high continuity), and where reflections are “weak,” uncertainty in interpretation increases. In general, enhancing image contrast helps to constrain the interpretation, as seen in the TWT image, where image contrast is three times that of the depth image and the fault placement population shows a narrower spread and shorter faults. A similar pattern is observed for reflection continuity, where high reflection continuity also results in a narrower fault placement spread and shorter fault interpretations. The differences in fault spread observed determine predicted fault heave, resulting, for example in regional sections, in significant differences in crustal stretching predictions. Further work to assess the relative contributions of contrast and continuity to visual image quality to create a single weighted parameter would provide a fully quantified visualization of image quality.

The two images were presented in different domains (TWT and depth), resulting in an 18% longer vertical scale in the depth image that could have changed the perception of the fault geometries to interpreters. However, our correlations suggest that image quality had the major influence on interpretation choice. We note that the average depth of the faults interpreted in the TWT image coincides with a boundary in depreciating image quality in the combined analysis. Although our results show that depth conversion choices (including the method used) change seismic image quality, all image manipulations have the potential to change interpretation outcomes. We therefore need to better understand image perception so that such image manipulations do not arbitrarily influence or bias interpretation outcome.

For a fixed binary threshold, image contrast and continuity are associated parameters, so increasing image contrast can artificially increase continuity. This correlation causes issues in determining the best methods for enhancing imagery in order to maximize interpretation effectiveness. It also has impacts on the processing of seismic data and the model chosen to create an image. Initial processing models generally assume a sub-horizontal, sub-parallel reflector stratigraphy with minimal disruption. Thus, they enhance reflector continuity. Our results, albeit based on TWT and depth imagery rather than different processing models, show that reflector continuity is spatially related to fault placement certainty. The processing of strong reflector continuity in seismic image data may result in greater constraint, or certainty, in fault placement than is warranted by the original data. Processing models must therefore be chosen carefully and interaction between the processor and the interpreter encouraged.

The results of the image analysis imply that there is a threshold at which seismic image data are too indeterminate (i.e., not enough contrast or continuity) to drive the interpretation. Quantitative image analysis could be used to determine the extent of an interpretation that is data-supported and areas that are more subjective. To create interpretations for under-constrained problems, reference models, such as fold or fault shape, can be employed. These reference models can be based on mechanical and geometric rules: e.g., angle of faulting, based on Andersonian mechanics (Anderson, 1905, 1951), or depth to detachment for faults (Chamberlin, 1910), based on mass balance principles (Dahlstrom, 1969; Elliott, 1983). Indeed, Bond et al. (2012) show that in areas of poor constraint, simple geological reasoning and reconstruction analysis can be used to reduce interpretation uncertainty. The method proposed in this work opens the door for a workflow for image quality assessment to indicate those occasions when model-based interpretation (e.g., fault geometry prediction at depth) may be more robust than the subjective fault interpretation of a geologist. Of course, these two approaches are complementary: image analysis may aid the interpreter in determining when geometric modeling may be useful and when interpretation uncertainty, and therefore potential risk, is high.

Even in the advent of more complex visualization through computing and screen technology, including the use of color and a greater pixel spectrum, interpretation uncertainty is determined by the quality of a seismic image. Understanding the impact of image quality on seismic interpretation using an 8-bit grayscale image provides a basis from which to investigate more complex aspects of visual perception, including color and luminescence. This work requires interdisciplinary research with cognitive scientists, neurologists, and others to fully understand how best to represent seismic imagery to maximize interpretation efforts.

A key finding of our experiments is that there are significant variations in the interpretation of fault geometries as depth increases in the section. This reflects the decay in image quality with depth. This uncertainty may be important—for example in picking the hanging-wall cut-offs of stratal reflectors on normal faults to correlate with those in the footwall that are otherwise well-imaged. This, in turn, influences determinations of fault heave—information that is critical for constructing maps that show fault linkages in sedimentary basins and for determining net extension of the upper crust. These inherent uncertainties arising from image quality are generally unreported in larger-scale studies of fault patterns. Therefore, the maps and net extension calculations used in many tectonic studies carry unknown errors.

## ACKNOWLEDGMENTS

BP/GUPCO are acknowledged for providing data from the Gulf of Suez. The authors acknowledge the support of MVE and use of Move software 2015.2 for this work. Ruediger Kilian is acknowledged for his kind help with the ImageJ code. Dr. Juan Alcalde is funded by NERC grant NE/M007251/1, on interpretational uncertainty. The work could not have been completed without the support of individuals within the geoscience community who took part in the interpretation experiment.

## REFERENCES CITED

Anderson, E.M., 1905, The dynamics of faulting: Transactions of the Edinburgh Geological Society, v. 8, p. 387–402, doi: 10.1144/transed.8.3.387.

Anderson, E.M., 1951, The Dynamics of Faulting and Dyke Formation with Application to Britain, Second Edition: Edinburgh, Oliver and Boyd, 206 p.

Badley, M.E., and Backshall, L.C., 1989, Inversion, reactivated faults and related structures: Seismic examples from the southern North Sea, *in* Cooper, M.A., and Williams, G.D., eds., Inversion Tectonics: Geological Society, London, Special Publication 44, p. 201–219, doi: 10.1144/GSL.SP.1989.044.01.12.

Bahorich, M., and Farmer, S., 1995, 3-D seismic discontinuity for faults and stratigraphic features: The coherence cube: The Leading Edge, v. 14, no. 10, p. 1053–1058, doi: 10.1190/1.1437077.

Baudon, C., and Cartwright, J., 2008, The kinematics of reactivation of normal faults using high resolution throw mapping: Journal of Structural Geology, v. 30, no. 8, p. 1072–1084, doi: 10.1016/j.jsg.2008.04.008.

Bond, C.E., Gibbs, D., Shipton, Z.K., and Jones, S., 2007, What do you think this is? “Conceptual uncertainty” in geoscience interpretation: GSA Today, v. 17, no. 11, p. 4–10, doi: 10.1130/GSAT01711A.1.

Bond, C.E., Lunn, R.J., Shipton, Z.K., and Lunn, A.D., 2012, What makes an expert effective at interpreting seismic images?: Geology, v. 40, no. 1, p. 75–78, doi: 10.1130/G32375.1.

Cartwright, J., and Huuse, M., 2005, 3D seismic technology: The geological “Hubble”: Basin Research, v. 17, no. 1, p. 1–20, doi: 10.1111/j.1365-2117.2005.00252.x.

Chamberlin, R.T., 1910, The Appalachian folds of central Pennsylvania: The Journal of Geology, v. 18, p. 228–251, doi: 10.1086/621722.

Cheng, M.-M., Zhang, G.-X., Mitra, N.J., Huang, X., and Hu, S.-M., 2011, Global contrast based salient region detection: Proceedings of the IEEE Computer Society Conference on Computer Vision and Pattern Recognition, article no. 5995344, p. 409–416.

Dahlstrom, C.D.A., 1969, Balanced cross sections: Canadian Journal of Earth Sciences, v. 6, p. 743–757, doi: 10.1139/e69-069.

Elliott, D., 1983, The construction of balanced cross-sections: Journal of Structural Geology, v. 5, p. 101.

Freeman, B., Yielding, G., and Badley, M., 1990, Fault correlation during seismic interpretation: First Break, v. 8, no. 3, p. 87–95.

Freeman, B., Quinn, D.J., Dillon, C.G., Arnhild, M., and Jaarsma, B., 2015, Predicting subseismic fracture density and orientation in the Gorm Field, Danish North Sea, *in* Richards, F.L., Richardson, N.J., Rippington, S.J., Wilson, R.W., and Bond, C.E., eds., Industrial Structural Geology: Principles, Techniques and Integration: Geological Society, London, Special Publication 421, p. 421–429.

Froner, B., Purves, S.J., Lowell, J., and Henderson, J., 2013, Perception of visual information: The role of colour in seismic interpretation: First Break, v. 31, no. 4, p. 29–34.

Gabrielsen, P.T., Abrahamson, P., Panzner, M., Fanavoll, S., and Ellingsrud, S., 2013, Exploring frontier areas using 2D seismic and 3D CSEM data, as exemplified by multi-client data over the Skrugard and Havis discoveries in the Barents Sea: First Break, v. 31, no. 1, p. 63–71.

Gao, D., 2009, 3D seismic volume visualization and interpretation: An integrated workflow with case studies: Geophysics, v. 74, no. 1, p. W1–W12, doi: 10.1190/1.3002915.

Hardy, S., 2015, The devil truly is in the detail. A cautionary note on computational determinism: Implications for structural geology numerical codes and interpretation of their results: Interpretation (Tulsa), v. 3, no. 4, p. SAA29–SAA35, doi: 10.1190/INT-2015-0052.1.

Heilbronner, R., and Barrett, S., 2013, Image Analysis in Earth Sciences: Microstructures and Textures of Earth Materials: Springer Science & Business Media, v. 129, 513 p.

Kadir, T., and Brady, M., 2001, Saliency, scale and image description: International Journal of Computer Vision, v. 45, no. 2, p. 83–105, doi: 10.1023/A:1012460413855.

Kim, Y., Varshney, A., Jacobs, D.W., and Guimbretiere, F., 2010, Mesh saliency and human eye fixations. ACM Transactions on Applied Perception, v. 7, no. 2, Article 12, February 2010, 13 pages, doi: 10.1145/1670671.1670676.

Kusznir, N.J., and Karner, G.D., 2007, Continental lithospheric thinning and breakup in response to upwelling divergent mantle flow: Application to the Woodlark, Newfoundland and Iberia margins, *in* Karner, G.D., Manatschal, G., and Pinheiro, L.M., eds., Imaging, Mapping and Modelling

Continental Lithosphere Extension and Breakup: Geological Society, London, Special Publication 282, p. 389–419, doi: 10.1144/SP282.16.
Platt, N.H., and Philip, P.R., 1995, Structure of the southern Falkland Islands continental shelf: Initial results from new seismic data: Marine and Petroleum Geology, v. 12, no. 7, p. 759–771, doi: 10.1016/0264-8172(95)93600-9.
Radonjić, A., Allred, S.R., Gilchrist, A.L., and Brainard, D.H., 2011, The dynamic range of human lightness perception: Current Biology, v. 21, no. 22, p. 1931–1936, doi: 10.1016/j.cub.2011.10.013.
Reynolds, J.H., and Desimone, R., 2003, Interacting roles of attention and visual salience in V4: Neuron, v. 37, no. 5, p. 853–863, doi: 10.1016/S0896-6273(03)00097-7.
Richards, F.L., Richardson, N.J., Bond, C.E., and Cowgill, M., 2015, Interpretational variability of structural traps: Implications for exploration risk and volume uncertainty, *in* Richards, F.L., Richardson, N.J., Rippington, S.J., Wilson, R.W., and Bond, C.E., eds., Industrial Structural Geology: Geological Society, London, Special Publication 421, p. 7–27.
Schneider, C.A., Rasband, W.S., and Eliceiri, K.W., 2012, NIH Image to ImageJ: 25 years of image analysis: Nature Methods, v. 9, p. 671–675, doi:10.1038/nmeth.2089.
Shaw, J.H., Connors, C., and Suppe, J., eds., 2005, Seismic interpretation of contractional fault-related folded: Tulsa, Oklahoma, AAPG Seismic Atlas: Studies in Geology, v. 53, p. 156.
Song, M., Tao, D., Chen, C., Li, X., and Chen, C.W., 2010, Color to gray: Visual cue preservation: IEEE Transactions on Pattern Analysis and Machine Intelligence, v. 32, no. 9, p. 1537–1552, doi: 10.1109/TPAMI.2009.74.
Thomson, K., and Underhill, J.R., 1999, Frontier exploration in the South Atlantic: Structural prospectivity in the North Falkland Basin: AAPG Bulletin, v. 83, no. 5, p. 778–797.
Underhill, J.R., and Paterson, S., 1998, Genesis of tectonic inversion structures: Seismic evidence for the development of key structures along the Purbeck-Isle of Wight Disturbance: Journal of the Geological Society, v. 155, no. 6, p. 975–992, doi: 10.1144/gsjgs.155.6.0975.
Wood, A.M., Paton, D.A., and Collier, R.E.L., 2015, The missing complexity in seismically imaged normal faults: What are the implications for geometry and production response? *in* Richards, F.L., Richardson, N.J., Rippington, S.J., Wilson, R.W., and Bond, C.E., eds., Industrial Structural Geology: Geological Society, London, Special Publication 421, p. 213–230.
Yielding, G., 2015, Trapping of buoyant fluids in fault-bound structures, *in* Richards, F.L., Richardson, N.J., Rippington, S.J., Wilson, R.W., and Bond, C.E., eds., Industrial Structural Geology: Geological Society, London, Special Publication 421, p. SP421–SP423.

Manuscript received 3 Feb. 2016
Revised manuscript received 8 Apr. 2016
Manuscript accepted 6 July 2016

# Call for Nominations
# GSA DIVISION AWARDS

**www.geosociety.org/divisions**

Give recognition where it is due—nominate a deserving colleague today! For award descriptions and nomination details, see the January issue of *GSA Today*, or visit **www.geosociety.org/divisions.**

## ARCHAEOLOGICAL GEOLOGY DIVISION

Nomination and application information for these three awards is at http://rock.geosociety.org/arch/.

**Rip Rapp Award**
**Nominations due** 15 Feb.
**Submit nominations to** Rolfe Mandel, mandel@ku.edu.

**Claude C. Albritton, Jr., Award**
**Nominations due** 5 March.
**Submit nominations to** gsa.agd@gmail.com.

**Richard Hay Student Paper/Poster Award**
**Nominations due** 20 Sept.
**Submit nominations to** gsa.agd@gmail.com.

## ENERGY GEOLOGY DIVISION

For more information about this and other Energy Geology Division awards (e.g., Distinguished Service, Best Paper), go to www.uky.edu/KGS/coal/GSA/awards.htm.

**Gilbert H. Cady Award**
**Nominations due** 28 Feb.
**Submit nominations to** Brett Valentine, bvalenti@vt.edu.

## ENVIRONMENTAL AND ENGINEERING GEOLOGY DIVISION

Nomination and application information for these and other E&EG Division awards (e.g., Meritorious Service, Distinguished Practice, Roy J. Shlemon Awards) is at http://community.geosociety.org/eegdivision/awards/about.

**Richard H. Jahns Distinguished Lecturer**
**Nominations due** 28 Feb.
**Submit nominations to** Thad Wasklewicz, wasklewiczt@ecu.edu (more information: http://community.geosociety.org/eegdivision/awards/jahns).

## GEOPHYSICS DIVISION

Nomination information is at http://community.geosociety.org/geophysicsdivision/home or www.geosociety.org/divisions/geop/Awards.htm.

**George P. Woollard Award**
**Nominations due** 15 Feb.
**Submit nominations to** Nick Schmerr, nschmerr@umd.edu.

## GEOSCIENCE EDUCATION DIVISION

Nomination information is at http://community.geosociety.org/gedivision/news/awards/biggsaward.

**Biggs Award for Excellence in Earth Science Teaching**
**Nominations due** 15 Feb.
**Submit nominations online;** direct questions to GEOEDGSA@gmail.com.

## HISTORY AND PHILOSOPHY OF GEOLOGY DIVISION

Nomination information for the following awards is at http://community.geosociety.org/histphildiv/awards.

**Mary C. Rabbitt History and Philosophy of Geology Award**
**Nominations due** 15 Feb.
**Submit nominations to** Kathleen Lohff, kathylohff@msn.com.

**Gerald M. and Sue T. Friedman Distinguished Service Award**
**Nominations due** 15 Feb.
**Submit nominations to** Kathleen Lohff, kathylohff@msn.com.

**History and Philosophy of Geology Student Award**
**Nominations due** 15 June
**Submit nominations to** Kathleen Lohff, kathylohff@msn.com.

## LIMNOGEOLOGY DIVISION

Nomination information is at http://community.geosociety.org/limnogeologydivision/home.

**Israel C. Russell Award**
**Nominations due** 1 March.
**Submit nominations to** David Finkelstein, finkelstein@hws.edu.

## MINERALOGY, GEOCHEMISTRY, PETROLOGY, AND VOLCANOLOGY (MGPV) DIVISION

Nomination information is at http://community.geosociety.org/mgpvdivision/awards.

**Nominations due** 31 March.
**Submit nominations to** J. Alex Speer, Mineralogical Society of America, 3635 Concorde Pkwy Suite 500, Chantilly, Virginia 20151-1110, USA; jaspeer@minsocam.org.

**MGPV Distinguished Geologic Career Award**

**MGPV Early Career Award**

### ■ QUATERNARY GEOLOGY AND GEOMORPHOLOGY

Nomination and application information is at http://community.geosociety.org/qggdivision/awards/awardsoverview.

**Farouk El-Baz Award for Desert Research**
**Nominations due** 1 April.

**Distinguished Career Award**
**Nominations due** 1 April.

### ■ SEDIMENTARY GEOLOGY DIVISION

Nomination information is at http://rock.geosociety.org/sed/SGD_Awards2.html#Sloss.

**Laurence L. Sloss Award for Sedimentary Geology**
**Nominations due** 1 March.
**Submit nominations to** Linda Kah, lckah@utk.edu.

### ■ SEDIMENTARY GEOLOGY DIVISION AND STRUCTURAL GEOLOGY AND TECTONICS DIVISION JOINT AWARD

Nomination information is at http://community.geosociety.org/sedimentarygeologydiv/awards/laubach.

**Stephen E. Laubach Structural Diagenesis Research Award**
**Nominations due** 1 April.
**Submit nominations to** Mark Evans, evansmaa@ccsu.edu.

### ■ STRUCTURAL GEOLOGY AND TECTONICS DIVISION

Nomination information is at http://rock.geosociety.org/sgt/.

**Career Contribution Award**
**Nominations due** 1 March.
More information: http://rock.geosociety.org/sgt/CareerAward.htm.

**Outstanding Publication Award**
**Nominations due** 1 March.
More information: http://rock.geosociety.org/sgt/BestPaperAward.htm.

# 2016 Outstanding Earth Science Teacher Awards

The National Association of Geoscience Teachers' Outstanding Earth Science Teacher Award recognizes excellence in earth-science teaching at the pre-college level. GSA awards the section recipients US$500 in travel money to attend a GSA meeting or to use for classroom supplies and complimentary membership in GSA for three years. State winners receive a one-year complimentary GSA membership.

## SECTION WINNERS

CENTRAL SECTION

**Troy J. Simpson**
Glenn Raymond School
Watseka, Illinois, USA

FAR WESTERN SECTION

**Laura Branch**
Ernest Righetti High School
Santa Maria, California, USA

MIDCONTINENT SECTION

**Will Squires**
Caddo Hills High School
Norman, Arkansas, USA

NEW ENGLAND SECTION

**Joan Kadaras**
Col. Moses Parker Middle School
Chelmsford, Massachusetts, USA

NORTH CENTRAL SECTION

**Sharla Hanzlik**
Niobrara High School
Niobrara, Nebraska, USA

PACIFIC NORTHWEST SECTION

**Jonathan Hill**
Marshfield High School
Coos Bay, Oregon, USA

SOUTHEASTERN SECTION

**Lindsay Knippenberg**
Mooresville Senior High School
Mooresville, North Carolina, USA

SOUTHWEST SECTION

**Matt Affolter**
Cottonwood High School
Salt Lake City, Utah, USA

TEXAS SECTION

**Sabrina Ewald**
Centennial High School
Frisco, Texas, USA

## STATE WINNERS

ALABAMA

**Kathryn Busby**
Tuscaloosa Magnet School Elementary
Tuscaloosa, Alabama, USA

ARIZONA

**Pradip Misra**
Bagdad High School
Bagdad, Arizona, USA

COLORADO

**Jessica Kindel**
Jefferson High School
Greeley, Colorado, USA

FLORIDA

**Mohamed Kabani**
Gordon Burnett Middle School
Seffner, Florida, USA

GEORGIA

**Stephen Csukas**
Tucker Middle School
Tucker, Georgia, USA

LOUISIANA

**Holly Payton**
Ruston Junior High School
Ruston, Louisiana, USA

MARYLAND

**Meaghan Richardson**
Connelly School of the Holy Child
Potomac, Maryland, USA

MINNESOTA

**Jody Bergeson**
Twin Bluff Middle School
Red Wing, Minnesota, USA

MISSISSIPPI

**Shelby J. "Dixie" Houchen**
Pearl Junior High School
Pearl, Mississippi, USA

NEW MEXICO

**Gary Bodman**
Eldorado High School
Albuquerque, New Mexico, USA

NORTH CAROLINA

**Lindsay Knippenberg**
Mooresville Senior High School
Mooresville, North Carolina, USA

OHIO

**DeAnn O'Toole**
Pattison Elementary School
Milford, Ohio, USA

OREGON

**Karen Shelton**
Central Middle School
Milton-Freewater, Oregon, USA

SOUTH CAROLINA

**Deborah Ezell**
Chesnee High School
Chesnee, South Carolina, USA

TENNESSEE

**John Griffin**
South Side High School
Jackson, Tennessee, USA

TEXAS

**Belinda Jacobs**
Cedar Ridge High School
Round Rock, Texas, USA

UTAH

**Kirk Wright**
Mt. Nebo Junior High
Payson, Utah, USA

WASHINGTON

**Dustin Smith**
Highlands Middle School
Kennewick, Washington, USA

The National Association
of Geoscience Teachers (NAGT)

Second Announcement

# SOUTHEASTERN SECTION

**66th Annual Meeting of the Southeastern Section, GSA**
**Richmond, Virginia, USA**
**30–31 March 2017**

**http://www.geosociety.org/se-mtg**

Lewis Ginter Botanical Garden. Photo used with permission from Richmond Region Tourism.

## *Rockin' the Fall Zone*

Strategically located on the Fall Zone, Richmond sits where the James River dramatically cascades over the Petersburg Granite at the eastern edge of the Piedmont to the sedimentary strata of the Coastal Plain. With either a stroll around town, or a short drive to the mountains or coast, Richmond is ideally located to explore the geologic diversity of the southeast. Technical Sessions will all be held at the Omni Richmond Hotel, 100 S. 12th Street, in Richmond.

### REGISTRATION

**Early registration deadline:** 27 Feb.
**Cancellation deadline:** 7 March
**Registration:** http://www.geosociety.org/GSA/Events/Section_Meetings/GSA/Sections/se/2017mtg/registration.aspx

**REGISTRATION FEES** (all fees are in U.S. dollars)

| Category | Early | | Standard | |
|---|---|---|---|---|
| | Full Meeting | One day | Full Meeting | One day |
| Professional member | $200 | $120 | $230 | $140 |
| Professional nonmember | $220 | $140 | $250 | $160 |
| Early Career Professional | $140 | $100 | $160 | $105 |
| Student member | $80 | $60 | $90 | $70 |
| Student nonmember | $90 | $80 | $120 | $90 |
| K–12 Professional | $40 | $40 | $50 | $40 |
| Guest | $50 | N/A | $50 | N/A |
| Field trip/workshop only | $40 | N/A | $40 | N/A |

### HOTEL RATES AND AMENITIES

**Hotel registration deadline:** 7 March

Blocks of rooms have been reserved at the Omni Richmond Hotel, located at 100 South 12th Street, Richmond, VA 23219, USA, +1-804-344-7000. The meeting will take place within the Omni Richmond's convention facilities. The meeting rate is US$165 per night plus tax for single and double occupancy. To make your reservations, please call Omni Reservations at 1-800-THE-OMNI and be sure to refer to the code: 17SEGSA. Omni guests are provided complimentary Wi-Fi access by joining the Omni Select Guest program. Omni guests will have access to the James Center YMCA.

### FIELD TRIPS

**Pre-Meeting**

1. **Geology along the Blue Ridge Parkway in Virginia.** 27–29 March. Cost: US$275 (min. 12/max. 28). Mark Carter, USGS, mcarter@usgs.gov; Scott Southworth, USGS, ssouthw@usgs.gov; Richard Tollo, GWU, rtollo@gwu.edu; Arthur Merschat, USGS; Sara Wagner, GWU; Ava Lazor, GWU; John Aleinikoff; USGS.
2. **From Laurentia to Iapetus: Traversing the Blue Ridge–Piedmont Terrane Boundary in Central Virginia.** 28–29 March. Cost: US$170 (min. 10/max. 22). Christopher M. Bailey, College of William and Mary, cmbail@wm.edu; Anna V. Spears, College of William and Mary, avspears@email.wm.edu; Aaron Marshall, College of William and Mary.
3. **Fossil-Collecting from the Middle Miocene Carmel Church Quarry Marine Ecosystem.** 29 March. Cost: US$70 (min. 8/max. 21). Alexander K. Hastings, Virginia Museum of Natural History, alexander.hastings@vmnh.virginia.gov; Ray Vodden, Virginia Museum of Natural History, raymond.vodden@vmnh.virginia.gov; Christina Byrd, Virginia Museum of Natural History, christina.byrd@vmnh.virginia.gov.
4. **Geology and Geomorphology of Belle Isle, Richmond.** 29 March. Cost: US$20 (min. 10/max. 22). Karen M. Layou, Reynolds Community College, KLayou@reynolds.edu; Brent Owens, College of William and Mary, beowen@wm.edu.

**Post-Meeting**

5. **Geologic Controls on Cave Development in the Burnsville Cove Area, Bath and Highland Counties, Virginia.** 31 March–2 April. Cost: US$300 (min. 8/max. 16). Christopher Swezey, USGS, cswezey@usgs.gov; John Haynes, James Madison University, haynesjx@jmu.edu; Phil Lucas, Virginia Speleological Survey; Rick Lambert, Virginia Speleological Survey.
6. **Tertiary Strata and Paleontology of the James River Region, Virginia.** 1–2 April. Cost: US$300 (min. 10/max. 25). Lauck W. Ward, Virginia Museum of Natural History, lauck.ward@vmnh.virginia.gov; Harry Dowsett, USGS.
7. **Geologic Evolution, Modern Processes, and Management Strategies of Virginia's Mainland Beaches and Barrier Islands.** 1–2 April. Cost: US$250 (min. 12/max. 24). Michael Fenster, Randolph Macon College, mfenster@rmc.edu; Christopher Hein, Virginia Institute of Marine Science, hein@vims.edu.
8. **Geology and Biostratigraphy of the Potomac River Cliffs at Stratford Hall, Westmoreland County, Virginia.** 1 April. Cost: US$95 (min. 15/max. 36). Rob Weems, USGS, rweems4@gmail.com; Lucy Edwards, USGS, leedward@usgs.gov; Bryan Landacre, USGS.
9. **Geology of the Petersburg Batholith, Eastern Piedmont, Virginia.** 1 April. Cost: US$70 (min. 10/max. 21). Brent Owens, College of William & Mary, beowen@wm.edu; Mark Carter, USGS, mcarter@usgs.gov; Christopher M. Bailey, College of William & Mary, cmbail@wm.edu.
10. **Geology and the Petersburg Campaign in the American Civil War.** 1 April. Cost: US$60 (min. 8/max. 22). C.R. Berquist, VDGMR, crberq@wm.edu; Marcie Occhi, VDGMR, marcie.occhi@dmme.virginia.gov; Aaron Cross, VDGMR, aaron.cross@dmme.virginia.gov; Jessica Strand, VDGMR.
11. **Industrial Minerals and Mines in the Arvonia Formation of the Chopawamsic Terrane, Buckingham County, Virginia.** 1 April. Cost: US$70 (min. 10/max. 21). Chee Saunders, Cardno Inc., chee.saunders@cardno.com.

## OPPORTUNITIES FOR STUDENTS AND EARLY CAREER PROFESSIONALS

### Mentor Programs

Questions? Contact Jennifer Nocerino at jnocerino@geosociety.org.

**Roy J. Shlemon Mentor Program in Applied Geoscience.** Students and early career professionals will have the opportunity to discuss career prospects and challenges with applied geoscientists from various sectors over a FREE lunch.

**John Mann Mentors in Applied Hydrology Program.** Students and early career professionals interested in applied hydrogeology or hydrology as a career will have the opportunity to network with professionals in these fields over a FREE lunch.

### Geoscience Career Workshops

**Part 1: Career Planning and Informational Interviewing**. Your job-hunting process should begin with career planning, not when you apply for jobs. This workshop will help you begin this process and will introduce you to informational interviewing.

**Part 2: Geoscience Career Exploration**. What do geologists in various sectors earn? What do they do? What are the pros and cons to working in academia, government, and industry? Workshop presenters, and when possible, professionals in the field, will address these issues.

**Part 3: Cover Letters, Résumés, and CVs.** How do you prepare a cover letter? Does your résumé need a good edit? Whether you are currently in the job market or not, learn how to prepare the best résumé possible. You will review numerous examples to help you learn important résumé dos and don'ts.

## LOCAL COMMITTEE

**General Co-Chairs:** David Spears, david.spears@dmme.virginia.gov; Karen Layou, klayou@reynolds.edu

**Technical Program Co-Chairs:** Beth McClellan, emcclellan@radford.edu; Mark Carter, mcarter@usgs.gov

**Field Trip Co-Chairs:** Chuck Bailey, cmbail@wm.edu; Shelley Jaye, sjaye@nvcc.edu

**Sponsorships Co-Chairs:** Steve Leslie, lesliea@jmu.edu; Matt Heller, matthew.heller@dmme.virginia.gov

**Exhibits Chair:** Chee Saunders, chee.saunders@cardno.com

**Student Volunteer Chair:** Lynsey Lemay, lemayl@tncc.edu

# GeoCareers—2017 Section Meetings

## GEOCAREERS

### Geoscience Career Workshops

For more information, contact Jennifer Nocerino at jnocerino@geosociety.org.

**Geoscience Career Workshop Part 1: Career Planning and Informational Interviewing.** Your job-hunting process should begin with career planning, not when you apply for jobs. This workshop will help you begin this process and will introduce you to informational interviewing.

**Geoscience Career Workshop Part 2: Geoscience Career Exploration.** What do geologists in various sectors earn? What do they do? What are the pros and cons?

**Geoscience Career Workshop Part 3: Cover Letters, Résumés, and CVs.** How do you prepare a cover letter? Does your résumé need a good edit? Learn how to prepare the best résumé possible and avoid typical pitfalls.

### Early Career Professional Focus Group

*(NE/NC and SC meetings only)*

Have you graduated in the last five years and are either a working professional or still looking for a job? GSA would like to support you in pursuing your professional goals. During this 45-minute session, participants will be asked a series of questions regarding potential programming and activities that GSA could offer to help you reach your goals. For more information, contact Tahlia Bear at tbear@geosociety.org.

## MENTOR PROGRAMS

Enjoy a free lunch while meeting with geoscience mentors working in the applied sector. The popularity of these programs means that space is limited, so plan to arrive early, because lunch is first-come, first-served. For further information, contact Jennifer Nocerino at jnocerino@geosociety.org.

**South-Central Section Meeting**
San Antonio, Texas, USA
Shlemon Mentor Luncheon Program: Mon., 13 March
Mann Mentors in Applied Hydrology Luncheon: Tues., 14 March

**Northeastern/North-Central Joint Meeting**
Pittsburgh, Pennsylvania, USA
Shlemon Mentor Luncheon Program: Mon., 20 March
Mann Mentors in Applied Hydrology Luncheon: Tues., 21 March

**Southeastern Section Meeting**
Richmond, Virginia, USA
Shlemon Mentor Luncheon Program: Thurs., 30 March
Mann Mentors in Applied Hydrology Luncheon: Fri., 31 March

**Cordilleran Section Meeting**
Honolulu, Hawaii, USA
Shlemon Mentor Luncheon Program: Tues., 23 May
Mann Mentors in Applied Hydrology Luncheon: Wed., 24 May

**Rocky Mountain Section Meeting**
Calgary, Alberta, Canada
Shlemon Mentor Luncheon Program: Fri., 9 June
Mann Mentors in Applied Hydrology Luncheon: Sat., 10 June

## MENTORING OPPORTUNITIES

**Professionals:** Interested in sharing information about your applied geoscience career with students? Being a mentor is a rewarding experience. If you can volunteer to mentor at one of the GSA Section Meetings, please contact Jennifer Nocerino at jnocerino@geosociety.org. *Early career professionals are encouraged to volunteer.*

# ELECTIONS: GSA OFFICERS and COUNCILORS

## GSA ELECTIONS BEGIN 17 MARCH 2017

GSA's success depends on you—its members—and the work of the officers serving on GSA's Executive Committee and Council. Members will receive instructions for accessing a member-only electronic ballot via our secure website, and biographical information on the nominees will be online for you to review at that time. Paper versions of both the ballot and candidate information will also be available upon request. Please help continue to shape GSA's future by voting on these nominees.

## 2017 OFFICER NOMINEES

| PRESIDENT | PRESIDENT-ELECT / PRESIDENT | TREASURER |
|---|---|---|
| (July 2017–June 2018) | (July 2017–June 2018) / (July 2018–June 2019) | (July 2017–June 2018) |
| **Isabel P. Montanez** | **Robbie R. Gries** | **Richard C. Berg** |
| University of California Davis | Gries Energy Partners LLC | Illinois State Geological Survey |
| Davis, California, USA | Lakewood, Colorado, USA | Champaign, Illinois, USA |
| *We congratulate our incoming president!* | | |

## 2017 COUNCIL NOMINEES

| COUNCILOR POSITION 1 | COUNCILOR POSITION 2 | COUNCILOR POSITION 3 |
|---|---|---|
| (July 2017–June 2021) | (July 2017–June 2021) | (July 2017–June 2021) |
| **Rónadh Cox** | **Joan E. Fryxell** | **Margaret R. Eggers** |
| Williams College | California State University San Bernardino | Eggers Environmental Inc. |
| Williamstown, Massachusetts, USA | San Bernardino, California, USA | Oceanside, California, USA |
| **Carmala N. Garzione** | **Michael L. Williams** | **Suzanne O'Connell** |
| University of Rochester | University of Massachusetts–Amherst | Wesleyan University |
| Rochester, New York, USA | Waltham, Massachusetts, USA | Middletown, Connecticut, USA |

To be counted, ballots must be submitted electronically, faxed to GSA Headquarters, or postmarked before midnight on 16 April 2017.

***CALL FOR NOMINATIONS***

## 2017–2018 GSA James B. Thompson, Jr., Distinguished International Lecturers

GSA International seeks nominations for distinguished geoscientist speakers for the 2017–2018 GSA James B. Thompson, Jr., Distinguished International Lecturer. Nominations are being accepted for two dynamic speakers of established scientific stature who can present stimulating and cutting-edge geoscience research for one or two tours each. The nominee(s) may be either living outside of North America and able to lecture at North American institutions or living within North America and be able to lecture internationally on topics that are at the forefront of research. The deadline to submit your nominations is **1 March 2017** (self-nominations are welcome).

**http://www.geosociety.org/Intl_LectureTour**

# Belt Basin
## Window to Mesoproterozoic Earth

***Edited by John S. MacLean and James W. Sears***

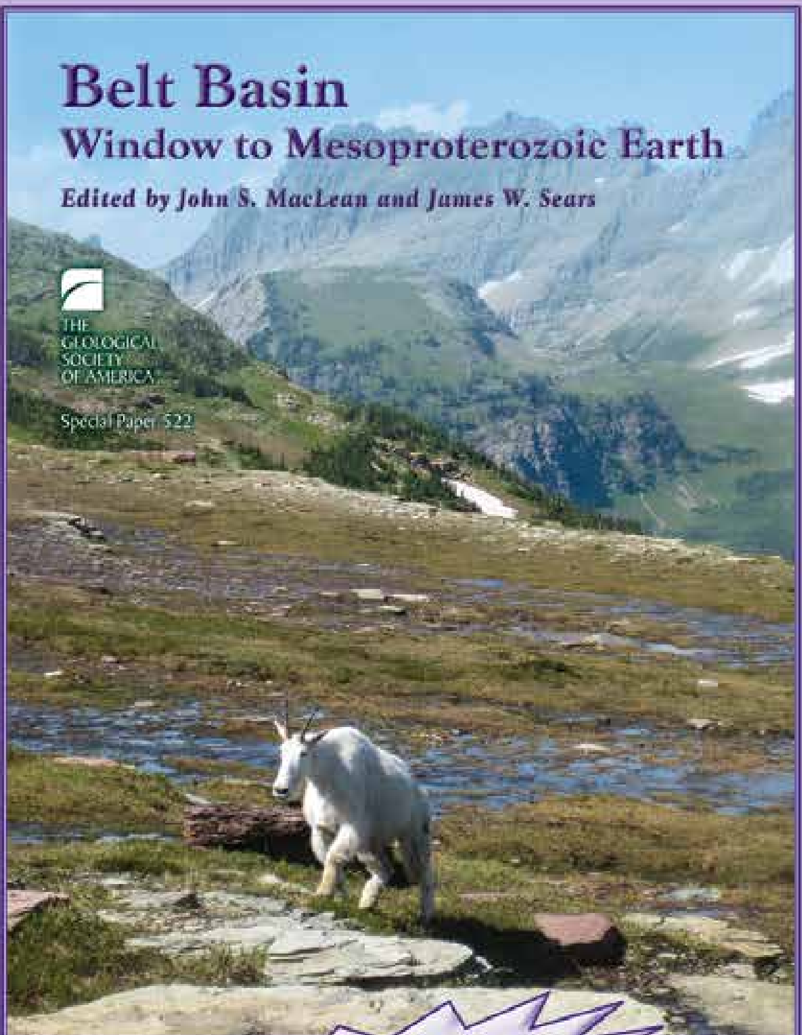


member price
**$56.00**

THE GEOLOGICAL SOCIETY OF AMERICA®

**SPECIAL PAPER 522**

With its thickness of more than 15 km of strata, covering some 200,000 km², the Belt Basin displays one of the planet's largest, best-exposed, most accessible, and best-preserved sequences of Mesoproterozoic sedimentary and igneous rocks. This volume focuses on research into this world-class province; kindles ideas about this critical era of Earth evolution; and covers aspects of the basin from its paleontology, mineralogy, sedimentology, and stratigraphy to its magmatism, ore deposits, geophysics, and structural geology.


SPE522, 384 p.
ISBN 9780813725222

$80.00, **member price $56.00**

toll-free 1.888.443.4472
1.303.357.1000, option 3
gsaservice@geosociety.org

***Buy online at http://rock.geosociety.org/store/***

Double Science Issue!

# Late Miocene Uplift of the Tian Shan and Altai and Reorganization of Central Asia Climate

# Late Miocene Uplift of the Tian Shan and Altai and Reorganization of Central Asia Climate

***Jeremy K. Caves****, *Earth System Science, Stanford University, Stanford, California 94305, USA;* ***Bolat U. Bayshashov,*** *Institute of Zoology, Academy of Sciences, Almaty 050060, Kazakhstan;* ***Aizhan Zhamangara,*** *L.N. Gumilyov Eurasian National University, Astana 01000, Kazakhstan;* ***Andrea J. Ritch, Daniel E. Ibarra,*** *Earth System Science, Stanford University, Stanford, California 94305, USA;* ***Derek J. Sjostrom,*** *Geology Program, Rocky Mountain College, Billings, Montana 59102, USA;* ***Hari T. Mix,*** *Environmental Studies and Sciences, Santa Clara University, Santa Clara, California 95053, USA;* ***Matthew J. Winnick,*** *Geological Sciences, Stanford University, Stanford, California 94305, USA; and* ***C. Page Chamberlain,*** *Earth System Science, Stanford University, Stanford, California 94305, USA*

## ABSTRACT

The timing of high surface topography and the corresponding climatic impacts of the many high ranges north of the Tibetan Plateau, such as the Altai and Tian Shan, remain poorly constrained. Most Neogene reconstructions of Central Asia climate come from interior China, where the influences of Altai and Tian Shan uplift are difficult to deconvolve from effects due to Tibetan Plateau uplift and changes in global climate. We present a new pedogenic carbonate oxygen and carbon isotope record from terrestrial Neogene sediments of the Zaysan Basin in eastern Kazakhstan, which lies upwind of the Altai and Tian Shan, in contrast to the numerous paleoclimate records from interior China. The $\delta^{18}O$ values of pedogenic carbonate exhibit a robust 4‰ decrease in the late Neogene—a trend that sharply contrasts with nearly all downwind records of $\delta^{18}O$ from Central Asia. We attribute this decrease to the establishment of the modern seasonal precipitation regime whereby Kazakhstan receives the majority of its moisture in the spring and fall, which lowers the $\delta^{18}O$ of pedogenic carbonates. The dominance of spring and fall precipitation in Kazakhstan results from the interaction of the mid-latitude jet with the high topography of the Altai and Tian Shan during its movement northward in spring and southward in fall. The late Miocene interaction of the jet with these actively uplifting northern Central Asia ranges reorganized Central Asia climate, establishing starkly different seasonal precipitation regimes, further drying interior China, and increasing the incidence of the lee cyclones that deposit dust on the Loess Plateau. We conclude that paleoclimatic changes in Central Asia in the Neogene are more tightly controlled by the interaction of the mid-latitude westerlies with the bounding ranges of northern Central Asia than by changes in the height or extent of the Tibetan Plateau.

## INTRODUCTION

Research on tectonic-climatic coupling in Asia has focused primarily on the importance of the Tibetan Plateau in strengthening monsoonal circulation and in aridifying Central Asia (Zhisheng et al., 2001; Zhang et al., 2007). However, recent work places Plateau uplift in the Paleogene (Rowley and Currie, 2006), challenging the mechanisms that couple Plateau orography with increasing Central Asian aridity in the Neogene (Molnar et al., 2010; Caves et al., 2016). In contrast, many of the high ranges north of the Plateau—including the Tian Shan and Altai—appear to have uplifted more recently (Charreau et al., 2009; De Grave et al., 2007), suggesting that they may play a role in the Neogene paleoclimatic history of Central Asia (Fig. 1). Today, these ranges cast substantial rain shadows, with substantially more precipitation on their windward flanks than in the lee deserts of the Gobi and Taklamakan (Fig. 2A). Further, these ranges demarcate a stark precipitation seasonality boundary, with dominantly spring and fall precipitation to the west and primarily summertime precipitation to the east (Fig. 2B) (Baldwin and Vecchi, 2016).

Unfortunately, there is little paleoclimatic data that unequivocally indicate when the surface topography of these ranges became sufficiently prominent to impact climate in Asia. Basin analysis and sedimentological data indicate that residual topography has continuously separated many of the inward-draining basins in Central Asia since the Mesozoic (Carroll et al., 2010). Thermochronological and sedimentological studies demonstrate that reactivation of Paleozoic structures in the Tian Shan and Altai began in the late Paleogene and accelerated and/or propagated northward by the late Miocene (Charreau et al., 2009; De Grave et al., 2007). However, most paleoclimatic records in Asia come from the arid expanses of interior China, where the competing influences of uplift, Paratethys retreat, and global climate are difficult to deconvolve (Sun et al., 2013; Tang et al., 2011; Molnar et al., 2010). General circulation models (GCMs) configured with paleo-boundary conditions also produce equivocal results because their relatively low resolution hinders proper treatment of Tian Shan and Altai uplift. Therefore, most work has focused on Tibetan Plateau uplift or westward retreat of the Paratethys (Zhisheng et al., 2001; Zhang et al., 2007).

To test when the Altai and Tian Shan became sufficiently prominent to impact climate, we collected pedogenic and lacustrine carbonates for isotopic analysis from the Zaysan Basin in Kazakhstan, a long-lived basin that lies windward of the Altai

*GSA Today*, v. 27, no. 2, doi: 10.1130/GSATG305A.1.
*Corresponding author: jeremy.caves@gmail.com; now at Earth Surface Dynamics, ETH Zürich, 8092 Zürich, Switzerland.

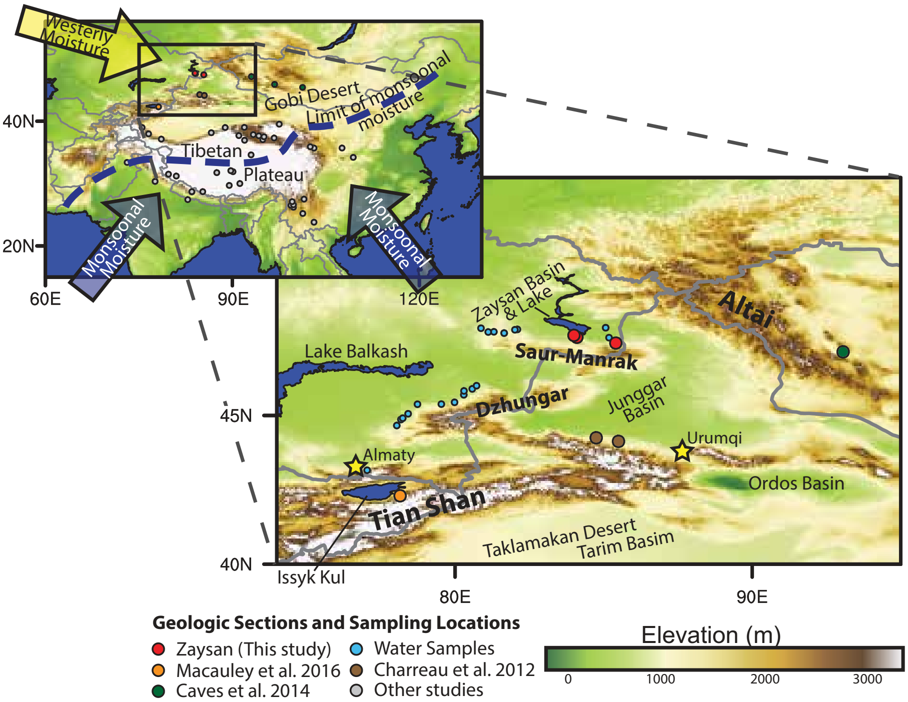


**Figure 1. Location map. Inset: yellow arrow—westerly moisture; blue arrows—monsoonal moisture. Dashed blue line—approximate, modern-day inland extent of monsoonal moisture (Araguás-Araguás et al., 1998).**

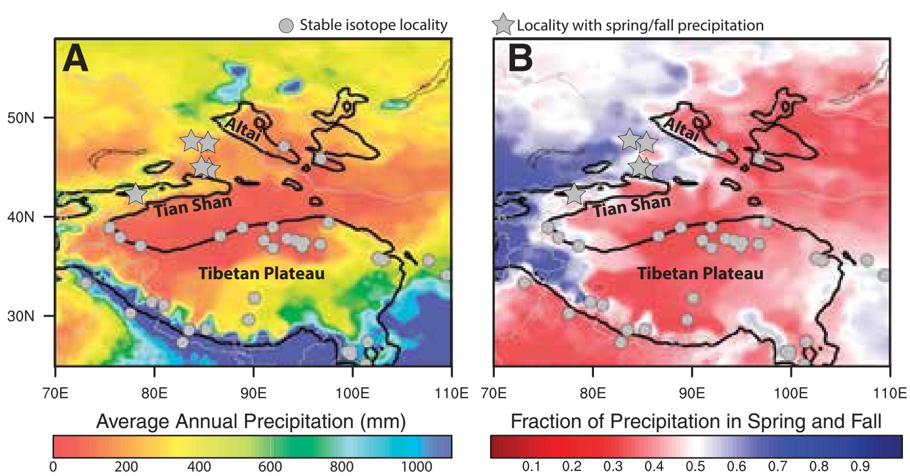


**Figure 2. (A) Average annual precipitation. (B) Fraction of precipitation that falls in spring and fall versus total spring-summer-fall precipitation. Data from the Global Precipitation Climatology Center (Meyer-Christoffer et al., 2015). Gray points—Neogene sedimentary stable isotope localities; gray stars—sites impacted by spring and fall precipitation seasonality; black line—smoothed 2000 m contour. Major ranges are labeled.**

and Tian Shan (Fig. 1). Oxygen isotopes ($\delta^{18}O$) are particularly sensitive to the effects of orographically forced rainout on the windward flanks of ranges (Mulch, 2016; Winnick et al., 2014), suggesting that any interaction between the Tian Shan and Altai and climate should be detectable in the Zaysan Basin. We find a 4‰ decrease in $\delta^{18}O$ in the late Neogene, which starkly contrasts with nearly all other records of sedimentary $\delta^{18}O$ from downwind localities in interior China and Mongolia that in general are constant or increasing during the Neogene (Caves et al., 2015). The timing of the $\delta^{18}O$ decrease in the Zaysan Basin is broadly synchronous with both accelerated uplift of the Tian Shan and Altai and Northern Hemisphere cooling. We attribute this decrease to a combination of sufficiently high topography and an equator-ward shift of the mid-latitude jet during cooling, which interact to create the modern spring and fall precipitation regime in Kazakhstan. The resulting climatic effects reorganized climate in Central Asia, further drying interior China and establishing the modern seasonal precipitation regime in Central Asia.

## GEOLOGIC AND CLIMATIC SETTING

The Zaysan Basin (48°N; 84°E) lies in eastern Kazakhstan, bordered to the north by the Altai and to the south and east by the Saur-Manrak ranges, which separate the Zaysan Basin from the Junggar Basin (Fig. 1). These ranges are the northern end of the Dzhungar Mountains, which splay northward off the Tian Shan northeast of Almaty. As Russell and Zhai (1987, p. 158) note, "Perhaps nowhere in Asia … is there a better sequence of continental Tertiary sediments than that found in the Zaysan Basin." Though more recent work suggests substantial unconformities, sediments in the basin represent nearly every epoch since the Late Cretaceous (Lucas et al., 2009). The Paleogene and early Neogene are primarily lacustrine, which transitions to pedogenic redbeds by the late Neogene (Lucas et al., 2000).

Climatically, the Zaysan Basin is exceptionally continental, with wintertime (DJF) temperatures less than −15 °C and summertime (JJA) mean daily temperatures nearing 20 °C (Schiemann et al., 2008) (Fig. 3). Moisture is supplied entirely by the mid-latitude westerlies (Fig. 4), because high ranges to the south, including the Tian Shan, Pamir, and Hindu Kush, block subtropical air from penetrating into Kazakhstan (Schiemann et al., 2008). Notably, the Zaysan Basin lies on the border between two contrasting precipitation regimes: Kazakhstan receives the majority of its precipitation in the spring (MAM) and fall (SON), whereas interior China and Mongolia experience dominantly JJA precipitation (Baldwin and Vecchi, 2016) (Fig. 2B). This pronounced difference in precipitation seasonality is a consequence of the annual migration of the Northern Hemisphere mid-latitude jet, which swings northward in April and returns

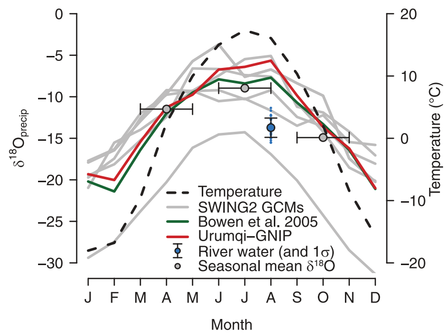


**Figure 3. Average $\delta^{18}O_p$ and surface air temperature (black, dashed line) (Mitchell and Jones, 2005) in the Zaysan Basin during the year. Gray lines—SWING2 general circulation model (GCM) experiments (Risi et al., 2012); gray points—precipitation-weighted seasonal $\delta^{18}O_p$ as estimated from the SWING2 data; dark green line—Online Precipitation Isotope Calculator (Bowen et al., 2005); red line—precipitation-weighted monthly means of $\delta^{18}O_p$ from the Urumqi Global Network of Isotopes in Precipitation (GNIP) site (IAEA/WMO, 2016); blue points—measured stream water $\delta^{18}O$ in Kazakhstan.**

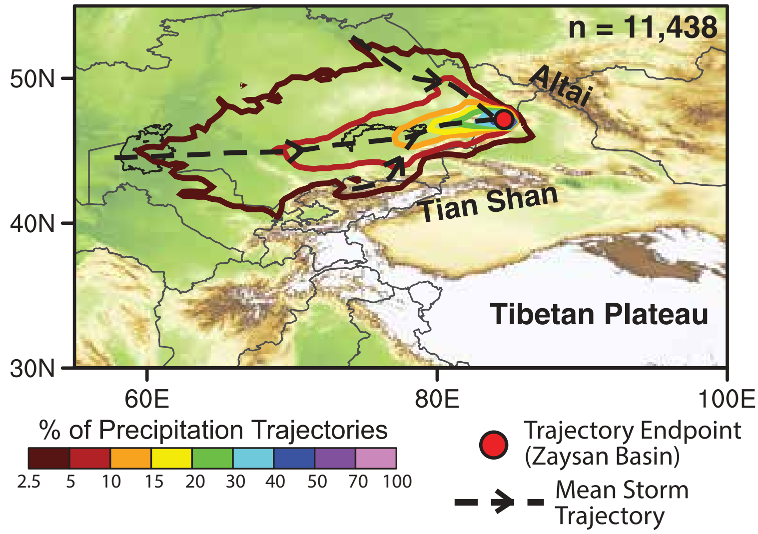


**Figure 4. 2-D histogram of storm trajectories between 2005 and 2015 that produced precipitation over the Zaysan Basin, mapped using the Hybrid Single-Particle Lagrangian Integrated Trajectory Model (HYSPLIT) (Stein et al., 2015) (see the GSA Supplemental Data Repository [text footnote 1] for further details). Dashed black lines with arrows—dominant storm trajectories to the Zaysan Basin (red point). Note that all precipitation-producing storms originate to the west of the Zaysan Basin and none traverse the high topography to the south.**

south in October (Schiemann et al., 2009). During this biannual migration, cyclones originating to the west interact with the Tian Shan and Altai, producing orographic precipitation (Schiemann et al., 2008, 2009; Baldwin and Vecchi, 2016).

To characterize the modern precipitation $\delta^{18}O$ ($\delta^{18}O_p$) in the Zaysan Basin, we rely upon three methods (Fig. 3). First, we interpolate estimates of $\delta^{18}O_p$ from the SWING2 (Stable Water Isotope Intercomparison Group 2) database, which uses isotopically enabled atmospheric GCMs ($n = 6$) to estimate $\delta^{18}O_p$ at ~2.5° × 2.5° resolution (Risi et al., 2012). Second, we use the Online Precipitation Isotope Calculator (Bowen et al., 2005). Third, we calculate flux-weighted $\delta^{18}O_p$ from the Urumqi, China, GNIP (Global Network of Isotopes in Precipitation) station (IAEA/WMO, 2016). All three methods produce a similar seasonal cycle, with the lowest $\delta^{18}O_p$ during DJF and the highest during JJA (Fig. 3). Average MAM and SON $\delta^{18}O_p$ is lower relative to JJA by 3.6 ± 2.3‰ and 6.8 ± 1.8‰ (1σ), respectively (gray points, Fig. 3). This seasonal cycle is characteristic of the continental air masses of Central Asia (Araguás-Araguás et al., 1998).

## GEOLOGIC SAMPLING AND METHODS

We collected 77 pedogenic carbonate samples from the type-section in the Zaysan Basin along the Kalmakpay River in the southeast of the basin (47.4°N; 84.4°E). The sediments in the basin are classified into svitas (Sv.; similar to, but not strictly identical to formation) (Borisov, 1963). The upper Neogene comprises ~200 m of pedogenically altered, carbonate-rich redbeds, including the lower Kalmakpay Sv. and the upper Karabulak Sv. Kalmakpay Sv. sediments are primarily mudstones that dip ~15° NE and are separated from the yellowish sands of the underlying, carbonate-poor Sarybulak Sv. by an unconformity (Fig. 5). The overlying Karabulak Sv. is coarser, with multiple pebble conglomerates and cross-bedded sandstones that cut into pedogenic facies, and dips ~10° NE. Throughout the basin, this sequence is capped by the "Gobi Conglomerate" (Berkey and Morris, 1923), which is a Quaternary deposit (Lucas et al., 2009), from which we collected five samples of carbonate-rich cement. We also collected 54 samples from the lower Miocene, carbonate-rich, lacustrine Akzhar Sv. from the Tayzhugen and Kyzylkain River sections (Lucas et al., 2009) in the southwest of the basin. We measured carbonate $\delta^{18}O$ and $\delta^{13}C$ ($\delta^{18}O_c$ and $\delta^{13}C_c$) on a Finnigan MAT Delta+ XL mass spectrometer at the Stable Isotope Biogeochemistry Laboratory (Stanford University, California, USA; see the GSA Supplemental Data Repository[1] for full methods).

The ages of these sediments are constrained by biostratigraphy and magnetostratigraphy. The Akzhar Sv. is assigned to the Shanwangian Asian Land Mammal Age (ALMA) (16.9–13.7 Ma), and the overlying Sarybulak Sv. is assigned to the Tunggurian ALMA (13.7–11.1 Ma) (Kowalski and Shevyreva, 1997). The Karabulak Sv. contains abundant "Hipparion" fauna, which is correlated with the latest Turolian (8.7–5.3 Ma; latest Baodean ALMA) (Sotnikova et al., 1997; Vangengeim et al., 1993; Lucas et al., 2009). The intervening Kalmakpay Sv. is not as clearly constrained by mammal fossils, yet is a separate unit from the overlying Karabulak Sv. Following Vangengeim et al. (1993) and Lucas et al. (2009), we therefore place the lower boundary in the

[1] GSA Supplemental Data Repository Item 2017024, containing methods, additional climatology, sedimentary, and diagenetic background and discussion, figures and tables, is online at http://www.geosociety.org/datarepository/2017/. If you have questions, please email gsatoday@geosociety.org.

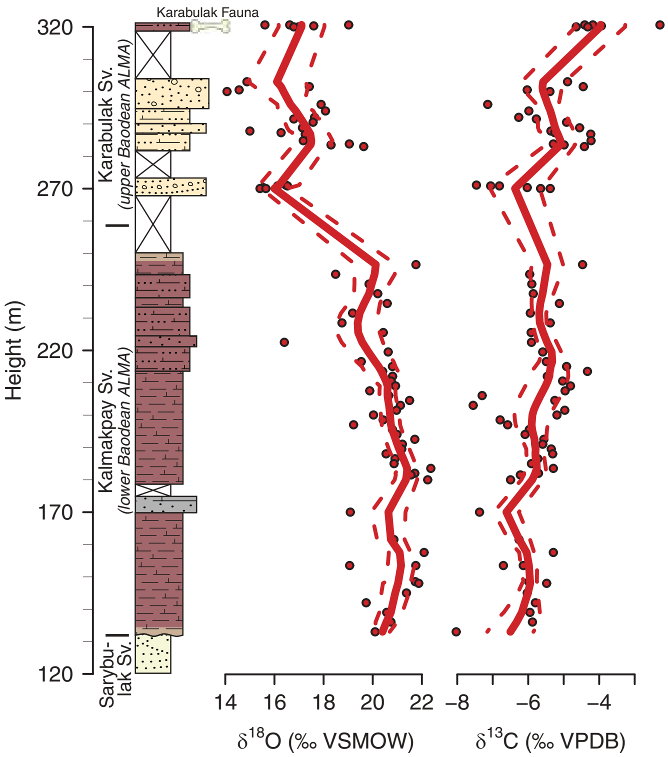


**Figure 5.** **δ18O and δ13C of pedogenic carbonates from the Kalmakpay River section against stratigraphic height. Solid and dashed red lines are a kernel-smooth of the data using an Epanechnikov kernel (mean and 1σ) with a 6 m bandwidth. Data from the overlying Gobi Conglomerate and underlying Akzhar Sv. are not shown (see Fig. 6). Sv.—svita; VSMOW—Vienna Standard Mean Ocean Water; VPDB—Vienna Pee Dee belemnite.**

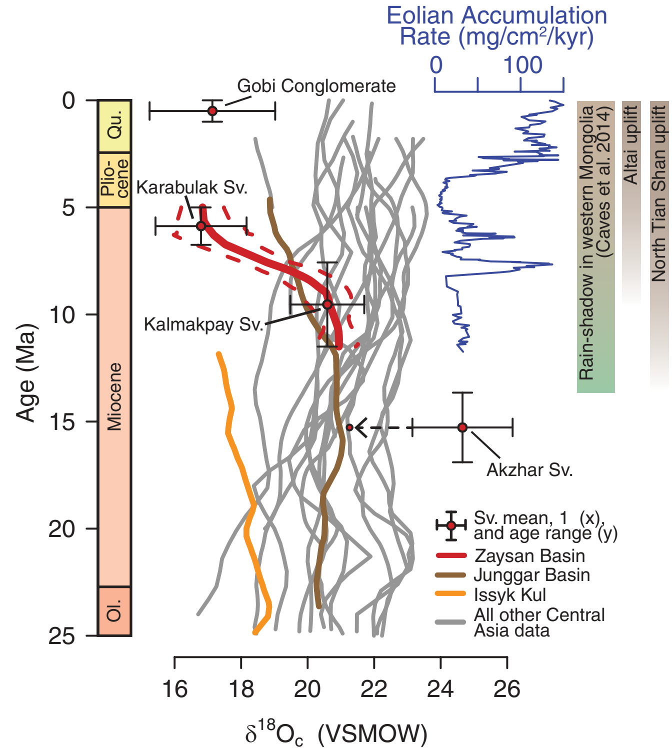


**Figure 6.** **δ18O data from Zaysan plotted against age. Red points are mean svita δ18O with 1σ uncertainty (*x*) and possible age range (*y*). Data from the Karabulak and Kalmakpay Sv. are smoothed using 1 Ma bandwidth Epanechnikov kernel (solid red line) with 1σ uncertainty (dashed red lines). Also plotted are published data from Central Asia (gray lines), Issyk Kul (orange line; Macaulay et al., 2016), and the Junggar Basin (brown line; Charreau et al., 2012). All are smoothed using an Epanechnikov kernel with 1 Ma bandwidth, after Caves et al. (2015). For the Akzhar Sv., we also plot the minimum δ18O value (small red point) due to evaporative enrichment in this svita. Eolian accumulation rate, as recorded by North Pacific deep-sea records (Rea et al., 1998), is a proxy for loess production. Note the prominent peak coincident with decreasing $\delta^{18}O_c$. Regional climatic and tectonic events are listed to the right. Shading indicates uncertainty in the timing of uplift and rain shadow development. Ol.—Oligocene; Qu.—Quaternary; Sv.—svita; VSMOW—Vienna Standard Mean Ocean Water.**

late Sarmatian (12.7–11.6 Ma) and the upper boundary in the lower Baodean ALMA. To account for the uncertainty in using this chronologic scheme, we present the data against both height (Fig. 5) and plotted against age (Fig. 6), where we bin the data by svita and assume that the sediments in each svita could have been deposited at any interval during the ALMA.

We also collected 29 stream and well-water samples to characterize the δ18O of modern waters in Kazakhstan. Stream waters integrate δ18O across storm and snowmelt events and are used to characterize modern water δ18O where $\delta^{18}O_p$ data are sparse (Hoke et al., 2014). We measured water δ18O on a Los Gatos Research TWIA-45EP liquid isotope water analyzer at Santa Clara University, California, USA.

## RESULTS

The mean Kalmakpay Sv. $\delta^{18}O_c$ (20.6‰) is significantly 4‰ higher than the mean $\delta^{18}O_c$ of the Karabulak Sv. (16.8‰) (Fig. 5). Similarly, there is a slight, but significant, increase in the mean $\delta^{13}C_c$ from the Kalmakpay Sv. (–5.8‰) to the Karabulak Sv. (–5.2‰). Using an estimate of the mean value (solid, red line in Fig. 5), $\delta^{13}C_c$ increases 2.5‰ from the base of the section to the top. The overlying Gobi Conglomerate samples have equivalent $\delta^{18}O_c$ as the underlying Karabulak samples, but higher $\delta^{13}C_c$.

Samples from the Akzhar Sv. show the greatest spread in $\delta^{13}C_c$ and $\delta^{18}O_c$ and the mean $\delta^{18}O_c$ (24.7‰) is significantly higher than the overlying svitas (see GSA supplemental data Table S1). Given the correlation between $\delta^{18}O_c$ and carbonate content (supplemental data Fig. S2), we treat these $\delta^{18}O_c$ data as evaporatively enriched. Following other studies in Central Asia (Rowley and Currie, 2006), we therefore consider the minimum $\delta^{18}O_c$ value as closest to the $\delta^{18}O_p$ value.

Stream/well water δ18O ranges from –15.5‰ to –11.3‰ (mean = –13.7‰) (supplemental data Table S2). This mean value is less than the estimated value of MAM $\delta^{18}O_p$ (–12.3‰) and substantially less than the estimated value of JJA $\delta^{18}O_p$ (–8.6‰). These samples were collected from streams that drain the 2500+ m Manrak-Saur-Dzhungar ranges and therefore likely integrate δ18O in catchments potentially still influenced by snowmelt and with large variations in elevation (Hoke et al., 2014).

## DISCUSSION

The most prominent trend in our record is the 4‰ decrease in $\delta^{18}O_c$ that occurs in the late Neogene. This trend is opposite to nearly all other $\delta^{18}O_c$ records in Central Asia that lie downwind of the Zaysan Basin and either increase or remain approximately constant over the Neogene (Fig. 6) (Caves et al., 2015). Notably, the only other records that decrease during the Neogene are those that also lie on the windward flank of the Tian Shan (Issyk Kul) and/or within the modern-day spring and fall precipitation regime (Junggar Basin) (gray stars; Fig. 2B).

What mechanisms might explain a simultaneous decrease in $\delta^{18}O$ on the windward flanks of the Tian Shan and Altai, while permitting constant or increasing $\delta^{18}O$ in their lee?

One potential mechanism is that increased orographic precipitation due to uplift might shift windward $\delta^{18}O$ to lower values, particularly as high-elevation precipitation is increasingly captured (Mulch, 2016). This hypothesis has been used to explain the decrease in $\delta^{18}O$ at both Issyk Kul and the Junggar Basin (Charreau et al., 2012; Macaulay et al., 2016). However, increased orographic precipitation appears unlikely to explain the full decrease in the Zaysan Basin. The long-term increase in $\delta^{13}C$ in the Zaysan Basin—at a location well north of where abundant $C_4$ vegetation is typically found (supplemental data Fig. S3)—indicates that soil respiration rates dropped, suggesting a decline in productivity and, hence, precipitation (Breecker et al., 2009; Caves et al., 2016). Further, increased orographic precipitation should also result in coupled $\delta^{18}O$ decreases in the lee of these ranges, which is not observed, though $\delta^{18}O_c$ in lee basins is complicated by evaporative effects (Mulch, 2016). An additional mechanism could be an increase in the formation temperature of pedogenic carbonate, given that the fractionation of $^{18}O$ between water and calcite decreases as temperature increases (~−0.2‰/°C) (Kim and O'Neil, 1997). However, an increase in temperature is unlikely because global climate cooled in the late Neogene following the Miocene Climatic Optimum (Zachos et al., 2001). Further, if changes in global temperature were the dominant factor driving changes in $\delta^{18}O_c$, one would expect similar decreases across much of northern Central Asia, which are not observed (Caves et al., 2015).

In contrast to the above two mechanisms, shifting precipitation seasonality in Kazakhstan might have a substantial effect on $\delta^{18}O_c$ given the large seasonal $\delta^{18}O_p$ changes observed in Central Asia (Fig. 3) (Araguás-Araguás et al., 1998). Pedogenic carbonates are seasonally biased recorders of $\delta^{18}O_p$, typically recording wet-season $\delta^{18}O_p$ (Breecker et al., 2009). Thus, a shift toward dominantly spring and fall precipitation might change the timing of pedogenic carbonate formation and decrease $\delta^{18}O_c$, without necessarily increasing total precipitation. Such a shift may have also lowered the temperature of carbonate formation, raising $\delta^{18}O_c$, and partially offsetting the true change in precipitation-weighted $\delta^{18}O_p$; this implies that the change in precipitation seasonality may have been substantial. Importantly, this change in precipitation seasonality would decouple windward $\delta^{18}O_c$ records (Zaysan, Issyk Kul, and Junggar) from leeward $\delta^{18}O_c$ records in interior China and Mongolia, which receive dominantly JJA precipitation.

## IMPLICATIONS

The modern spring and fall precipitation regime in Kazakhstan is a result of the interaction between cyclones routed along the mid-latitude westerly jet as it migrates seasonally north and south and the high topography of the Tian Shan and Altai (Schiemann et al., 2009). Thus, a change in precipitation seasonality would imply either a shift of the mid-latitude jet, the development of high topography, or both. The mean position of the jet is thought to have been farther northward during the late Miocene given warmer Arctic temperatures (Micheels et al., 2011), suggesting that cooling into the late Miocene may have contributed to a southward shift of the jet.

Further, northward growth of high topography in Asia would result in increased interaction between cyclones routed along the jet and this topography, resulting in orographic precipitation during the spring and fall (Baldwin and Vecchi, 2016). There is substantial evidence that deformation from the collision of India-Asia has propagated northward during the Cenozoic, resulting in—most recently in the latest Miocene—uplift of the Altai range (De Grave et al., 2007). The Altai rain shadow likely formed by the latest Miocene, as indicated by a substantial increase in pedogenic carbonate $\delta^{13}C$ in the lee of the Altai (Caves et al., 2014) (Fig. 6). In the northern Tian Shan, Charreau et al. (2009) found increased sedimentation rates in the Junggar Basin at ca. 11 Ma, which they proposed resulted from an acceleration of uplift. Though the individual uplift histories of the local Saur-Manrak ranges are unknown, but are likely linked to uplift in the Altai or northern Tian Shan (Campbell et al., 2013), we propose that the timing of this accelerated uplift is broadly synchronous with our observed decrease in $\delta^{18}O_c$. Northward-propagating deformation might also explain why oxygen isotopic records from Issyk Kul, which lies 5° south, decline starting in the early Miocene, reflecting earlier growth of high topography to the south (Macaulay et al., 2016).

Our new oxygen isotope record from the windward side of the Tian Shan and Altai ranges indicates that these ranges were sufficiently elevated by the late Miocene to impact climate in Central Asia. Most notably, this interaction resulted in a substantial reorganization of Central Asia climate, creating a stark precipitation seasonality boundary between eastern and western Central Asia. Such high topography would have further blocked moisture from reaching downwind Central Asia, contributing to the increasingly arid conditions and formation of the Taklamakan and Gobi deserts in the late Miocene (Caves et al., 2016; Sun et al., 2009). The Altai are the largest source of lee cyclones in Asia (Chen et al., 1991), and the combined interaction of high topography with the jet's oscillations as it moves northward in the spring (Schiemann et al., 2009) creates the dust storms that blanket the Loess Plateau (Shao and Dong, 2006; Roe, 2009). Thus, acceleration of loess deposition in the late Miocene (Zhang et al., 2014; Rea et al., 1998) may be a consequence of increasing cyclogenesis as a result of upwind topographic growth (Caves et al., 2014; Shi et al., 2015) (Fig. 6). The subsequent Pliocene decline in eolian accumulation rates may reflect a northward shifted jet during the mid-Pliocene Warm Period, which precluded interaction with the Altai until Quaternary cooling shifted the jet southward again.

We conclude that uplift of the Tian Shan and Altai reorganized late Neogene climate in Central Asia, establishing a prominent seasonal precipitation boundary as a result of increasing interactions between the mid-latitude jet and high topography. Thus, paleoclimatic changes in Central Asia in the late Neogene may not be due solely to changes in the extent or height of the Tibetan Plateau. In contrast, the timing of uplift and consequent climatic impacts of Asia's northern bounding ranges are critical to unraveling the paleoenvironmental history of Central Asia. Ultimately, future work to test this interpretation must include westward/upwind records of $\delta^{18}O$ combined with GCM studies that resolve the impact of Tian Shan and Altai uplift on Asian climate.

## ACKNOWLEDGMENTS

We thank our field expedition members, including B. Dautaliev, G. Nazyanbeteva, S. Samzatbaeva, J. Buztsev, and S. Bayshashov, and N. Ballantine, D. Moragne, and P. Blisniuk for assistance with lab work. We also thank two anonymous reviewers and editor G. Dickens for comments that improved the manuscript. A GSA Student Research grant (Caves), three Stanford University McGee grants (Caves, Ritch, and Ibarra), and NSF grants EAR-1009721 and EAR-1423967 (Chamberlain) funded this work. Caves is also funded by an NSF Graduate Research Fellowship (DGE-1147470) and a Stanford Graduate Fellowship.

## REFERENCES CITED

Araguás-Araguás, L., Froehlich, K., and Rozanski, K., 1998, Stable isotope composition of precipitation over southeast Asia: Journal of Geophysical Research, v. 103, D22, p. 28,721–28,742, doi: 10.1029/98JD02582.

Baldwin, J., and Vecchi, G., 2016, Influence of the Tianshan Mountains on arid extratropical Asia: Journal of Climate, v. 29, p. 5741–5762, doi: 10.1175/JCLI-D-15-0490.1.

Berkey, C.P., and Morris, F.K., 1923, Geology of Mongolia—A Reconnaissance Report Based on the Investigations of the Years 1922–1923: New York, American Museum of Natural History, 475 p.

Borisov, B.A., 1963, [The stratigraphy of the Upper Cretaceous and of the Paleogene-Neogene of the Zaysan Depression] Stratigrafiya verkhnego mela i paleogen-neogena Zaysanskoy vvpadiny. Materiali po geologii i poleznym iskopayemym Altaya i Kazakhstana: Trudy VSEGEI i Gos: Geol. Komenta, v. 94, p. 11–75.

Bowen, G.J., Wassenaar, L.I., and Hobson, K.A., 2005, Global application of stable hydrogen and oxygen isotopes to wildlife forensics: Oecologia, v. 143, no. 3, p. 337–348, doi: 10.1007/s00442-004-1813-y.

Breecker, D.O., Sharp, Z.D., and McFadden, L.D., 2009, Seasonal bias in the formation and stable isotopic composition of pedogenic carbonate in modern soils from central New Mexico, USA: GSA Bulletin, v. 121, no. 3–4, p. 630–640, doi: 10.1130/B26413.1.

Campbell, G.E., Walker, R.T., Abdrakhmatov, K., Schwenninger, J., Jackson, J., Elliott, J.R., and Copley, A., 2013, The Dzhungarian fault: Late Quaternary tectonics and slip rate of a major right-lateral strike-slip fault in the northern Tien Shan region: Journal of Geophysical Research, Solid Earth, v. 118, no. 10, p. 5681–5698, doi: 10.1002/jgrb.50367.

Carroll, A.R., Graham, S.A., and Smith, M.E., 2010, Walled sedimentary basins of China: Basin Research, v. 22, no. 1, p. 17–32, doi: 10.1111/j.1365-2117.2009.00458.x.

Caves, J.K., Sjostrom, D.J., Mix, H.T., Winnick, M.J., and Chamberlain, C.P., 2014, Aridification of Central Asia and uplift of the Altai and Hangay Mountains, Mongolia: Stable isotope evidence: American Journal of Science, v. 314, no. 8, p. 1171–1201, doi: 10.2475/08.2014.01.

Caves, J.K., Winnick, M.J., Graham, S.A., Sjostrom, D.J., Mulch, A., and Chamberlain, C.P., 2015, Role of the westerlies in Central Asia climate over the Cenozoic: Earth and Planetary Science Letters, v. 428, p. 33–43, doi: 10.1016/j.epsl.2015.07.023.

Caves, J.K., Moragne, D.Y., Ibarra, D.E., Bayshashov, B.U., Gao, Y., Jones, M.M., Zhamangara, A., Arzhannikova, A.V., Arzhannikov, S.G., and Chamberlain, C.P., 2016, The Neogene de-greening of Central Asia: Geology, v. 44, no. 11, p. 887–890, doi: 10.1130/G38267.1.

Charreau, J., Chen, Y., Gilder, S., Barrier, L., Dominguez, S., Augier, R., Sen, S., Avouac, J.-P., Gallaud, A., Graveleau, F., and Wang, Q., 2009, Neogene uplift of the Tian Shan Mountains observed in the magnetic record of the Jingou River section (northwest China): Tectonics, v. 28, no. 2, TC2008, doi: 10.1029/2007TC002137.

Charreau, J., Kent-Corson, M.L., Barrier, L., Augier, R., Ritts, B.D., Chen, Y., France-Lannord, C., and Guilmette, C., 2012, A high-resolution stable isotopic record from the Junggar Basin (NW China): Implications for the paleo-topographic evolution of the Tianshan Mountains: Earth and Planetary Science Letters, v. 341–344, p. 158–169, doi: 10.1016/j.epsl.2012.05.033.

Chen, S., Kuo, Y., Zhang, P., and Bai, Q., 1991, Synoptic climatology of cyclogenesis over East Asia, 1958–1987: Monthly Weather Review, v. 119, p. 1407–1418, doi: 10.1175/1520-0493(1991)119<1407:SCOCOE>2.0.CO;2.

De Grave, J., Buslov, M.M., and van den Haute, P., 2007, Distant effects of India–Eurasia convergence and Mesozoic intracontinental deformation in Central Asia: Constraints from apatite fission-track thermochronology: Journal of Asian Earth Sciences, v. 29, no. 2–3, p. 188–204, doi: 10.1016/j.jseaes.2006.03.001.

Hoke, G.D., Liu-Zeng, J., Hren, M.T., Wissink, G.K., and Garzione, C.N., 2014, Stable isotopes reveal high southeast Tibetan Plateau margin since the Paleogene: Earth and Planetary Science Letters, v. 394, p. 270–278, doi: 10.1016/j.epsl.2014.03.007.

IAEA/WMO, 2016, Global Network of Isotopes in Precipitation: The GNIP Database: http://www.iaea.org/water.

Kim, S., and O'Neil, J., 1997, Equilibrium and nonequilibrium oxygen isotope effects in synthetic carbonates: Geochimica et Cosmochimica Acta, v. 61, no. 16, p. 3461–3475, doi: 10.1016/S0016-7037(97)00169-5.

Kowalski, K., and Shevyreva, N.S., 1997, *Gliridae* (Mammalia: Rodentia) from the Miocene of the Zaisan Depression (Eastern Kazakhstan): Acta Zoologica Cracoviensia, v. 40, no. 2, p. 199–208.

Lucas, S.G., Aubekerov, B.Z., Dzhamangaraeva, A., Bayshashov, B.U., and Tyutkova, L.A., 2000, Cenozoic lacustrine deposits of the Ili Basin, southeastern Kazakhstan, *in* Gierlowski-Kordesch, E., and Kelts, K., eds., Lake Basins through Space and Time: AAPG Studies in Geology, v. 46, p. 59–64.

Lucas, S.G., Emry, R.J., Bayshashov, B., and Tyutkova, L., 2009, Cenozoic mammalian biostratigraphy and biochronology in the Zaysan Basin, Kazakstan: Museum of Northern Arizona Bulletin, v. 65, p. 621–634.

Macaulay, E.A., Sobel, E.R., Mikolaichuk, A., Wack, M., Gilder, S.A., Mulch, A., Fortuna, A.B., Hynek, S., and Apayarov, F., 2016, The sedimentary record of the Issyk Kul basin, Kyrgyzstan: Climatic and tectonic inferences: Basin Research, v. 28, p. 57–80, doi: 10.1111/bre.12098.

Meyer-Christoffer, A., Becker, A., Finger, P., Rudolf, B., Schneider, U., and Ziese, M., 2015, GPCC Climatology Version 2015 at 0.25°: Monthly land-surface precipitation climatology for every month and the total year from rain-gauges built on GTS-based and historic data: Global Precipitation Climatology Centre (GPCC) at Deutscher Wetterdienst, http://gpcc.dwd.de/, doi: 10.5676/DWD_GPCC/CLIM_M_V2015_025.

Micheels, A., Bruch, A.A., Eronen, J., Fortelius, M., Harzhauser, M., Utescher, T., and Mosbrugger, V., 2011, Analysis of heat transport mechanisms from a Late Miocene model experiment with a fully coupled atmosphere–ocean general circulation model: Palaeogeography, Palaeoclimatology, Palaeoecology, v. 304, no. 3–4, p. 337–350, doi: 10.1016/j.palaeo.2010.09.021.

Mitchell, T.D., and Jones, P.D., 2005, An improved method of constructing a database of monthly climate observations and associated high-resolution grids: International Journal of Climatology, v. 25, no. 6, p. 693–712, doi: 10.1002/joc.1181.

Molnar, P., Boos, W.R., and Battisti, D.S., 2010, Orographic controls on climate and paleoclimate of Asia: Thermal and mechanical roles for the Tibetan Plateau: Annual Review of Earth and Planetary Sciences, v. 38, no. 1, p. 77–102, doi: 10.1146/annurev-earth-040809-152456.

Mulch, A., 2016, Stable isotope paleoaltimetry and the evolution of landscapes and life: Earth and Planetary Science Letters, v. 433, p. 180–191, doi: 10.1016/j.epsl.2015.10.034.

Rea, D.K., Snoeckx, H., and Joseph, L.H., 1998, Late Cenozoic eolian deposition in the North Pacific: Asian drying, Tibetan uplift, and cooling of the northern hemisphere: Paleoceanography, v. 13, no. 3, p. 215–224, doi: 10.1029/98PA00123.

Risi, C., and 29 others, 2012, Process-evaluation of tropospheric humidity simulated by general circulation models using water vapor isotopologues: 1. Comparison between models and observations: Journal of Geophysical Research, D, Atmospheres, v. 117, no. 5, D05303, doi: 10.1029/2011JD016621.

Roe, G., 2009, On the interpretation of Chinese loess as a paleoclimate indicator: Quaternary Research, v. 71, no. 2, p. 150–161, doi: 10.1016/j.yqres.2008.09.004.

Rowley, D.B., and Currie, B.S., 2006, Palaeo-altimetry of the late Eocene to Miocene Lunpola basin, central Tibet: Nature, v. 439, p. 677–681, doi: 10.1038/nature04506.

Russell, D., and Zhai, R., 1987, The Paleogene of Asia: Mammals and Stratigraphy: Paris Museum National d'Histoire Naturelle, v. 2, 488 p.

Schiemann, R., Lüthi, D., Vidale, P.L., and Schär, C., 2008, The precipitation climate of Central Asia—Intercomparison of observational and numerical data sources in a remote semiarid region: International Journal of Climatology, v. 28, p. 295–314, doi: 10.1002/joc.1532.

Schiemann, R., Lüthi, D., and Schär, C., 2009, Seasonality and interannual variability of the westerly jet in the Tibetan Plateau region: Journal of Climate, v. 22, no. 11, p. 2940–2957, doi: 10.1175/2008JCLI2625.1.

Shao, Y., and Dong, C.H., 2006, A review on East Asian dust storm climate, modelling and monitoring: Global and Planetary Change, v. 52, p. 1–22, doi: 10.1016/j.gloplacha.2006.02.011.

Shi, Z., Liu, X., Liu, Y., Sha, Y., and Xu, T., 2015, Impact of Mongolian Plateau versus Tibetan Plateau on the westerly jet over North Pacific Ocean: Climate Dynamics, v. 44, p. 3067–3076, doi: 10.1007/s00382-014-2217-2.

Sotnikova, M., Dodonov, A., and Pen'kov, A., 1997, Upper Cenozoic bio-magnetic stratigraphy of Central Asian mammalian localities: Palaeogeography, Palaeoclimatology, Palaeoecology, v. 133, p. 243–258, doi: 10.1016/S0031-0182(97)00078-3.

Stein, A.F., Draxler, R.R., Rolph, G.D., Stunder, B.J.B., Cohen, M.D., and Ngan, F., 2015, NOAA's HYSPLIT atmospheric transport and dispersion modeling system: Bulletin of the American Meteorological Society, v. 96, p. 2059–2077, doi: 10.1175/BAMS-D-14-00110.1.

Sun, J., Zhang, Z., and Zhang, L., 2009, New evidence on the age of the Taklimakan Desert: Geology, v. 37, no. 2, p. 159–162, doi: 10.1130/G25338A.1.

Sun, J., Lü, T., Gong, Y., Liu, W., Wang, X., and Gong, Z., 2013, Effect of aridification on carbon isotopic variation and ecologic evolution at 5.3 Ma in the Asian interior: Earth and Planetary Science Letters, v. 380, p. 1–11, doi: 10.1016/j.epsl.2013.08.027.

Tang, Z., Ding, Z., White, P.D., Dong, X., Ji, J., Jiang, H., Luo, P., and Wang, X., 2011, Late Cenozoic central Asian drying inferred from a palynological record from the northern Tian Shan: Earth and Planetary Science Letters, v. 302, no. 3–4, p. 439–447, doi: 10.1016/j.epsl.2010.12.042.

Vangengeim, E.A., Vislobokova, I.A., Godina, A.Y., Dimitrieva, E.L., Zhegallo, V.I., Sotnikova, M.V., and Tleuberdina, P.A., 1993, On the age of mammalian fauna from the Karabulak Formation of the Kalmakpai River (Zaisan Depression, Eastern Kazakhstan): Stratigraphy and Geological Correlation, v. 1, no. 2, p. 165–171.

Winnick, M.J., Chamberlain, C.P., Caves, J.K., and Welker, J.M., 2014, Quantifying the isotopic "continental effect": Earth and Planetary Science Letters, v. 406, p. 123–133, doi: 10.1016/j.epsl.2014.09.005.

Zachos, J., Pagani, M., Sloan, L., Thomas, E., and Billups, K., 2001, Trends, rhythms, and aberrations in global climate 65 Ma to present: Science, v. 292, p. 686–693, doi: 10.1126/science.1059412.

Zhang, Z., Huijun, W., Zhengtang, G., and Dabang, J., 2007, Impacts of tectonic changes on the reorganization of the Cenozoic paleoclimatic patterns in China: Earth and Planetary Science Letters, v. 257, no. 3–4, p. 622–634, doi: 10.1016/j.epsl.2007.03.024.

Zhang, Y., Sun, D., Li, Z., Wang, F., Wang, X., Li, B., Guo, F., and Wu, S., 2014, Cenozoic record of aeolian sediment accumulation and aridification from Lanzhou, China, driven by Tibetan Plateau uplift and global climate: Global and Planetary Change, v. 120, p. 1–15, doi: 10.1016/j.gloplacha.2014.05.009.

Zhisheng, A., Kutzbach, J.E., Prell, W.L., and Porter, S.C., 2001, Evolution of Asian monsoons and phased uplift of the Himalaya-Tibetan plateau since Late Miocene times: Nature, v. 411, 6833, p. 62–66, doi: 10.1038/35075035.



Manuscript received 2 June 2016
Revised manuscript received 5 Sept. 2016
Manuscript accepted 21 Sept. 2016


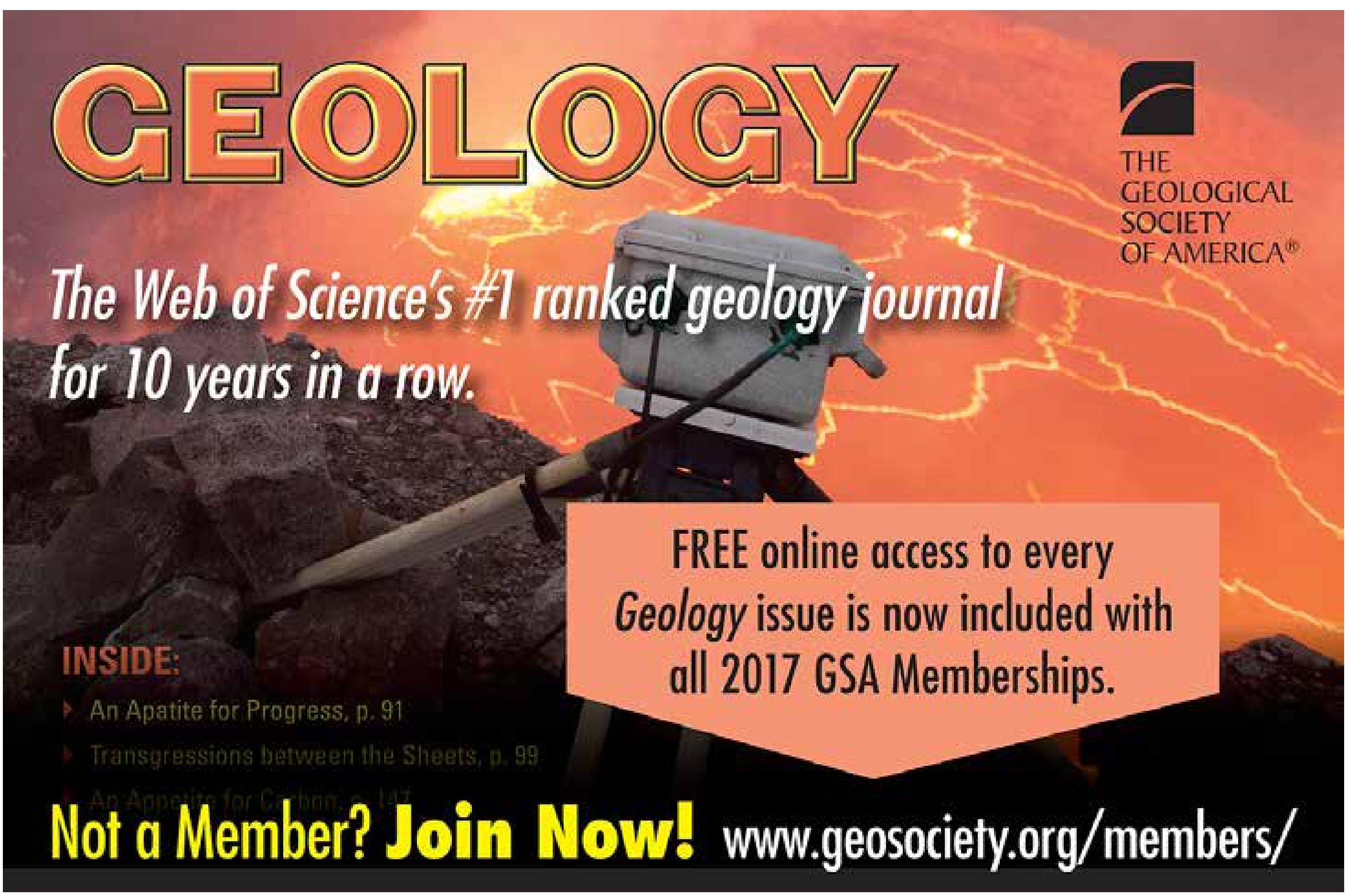

### Positions Open

**FACULTY POSITION**
**STRUCTURAL GEOLOGY AND**
**NEOTECTONICS, LAMAR UNIVERSITY**

The Department of Earth and Space Sciences, Lamar University, Beaumont, Texas is inviting applications for a tenure-track Assistant Professor to Associate position depending on qualifications. Beaumont is a community of approximately 117,000 people, located in Southeast Texas, 90 minutes from Houston and Johnson Space Center and 30 miles from the Louisiana border. Being 20 miles north of the Gulf of Mexico, southeast Texas has a balmy subtropical climate. The Department of Earth and Space Sciences engages in a breadth of research activities including geophysics, GIS, coastal processes, stratigraphy, paleontology, and planetary science. The department homes the Lamar Geospatial Center (LGC), a state-of-the art GIS center running ESRI products. The LGC also runs high-end geophysical software, including Petrel and Kingdom Suite. The Department also has membership in UNAVCO and IRIS.

We seek a person with primary interest in structural geology and neotectonics. Knowledge and experience in GIS is also highly desirable. Responsibilities include teaching structural and physical geology as well as co-teaching of field camp. Minimum qualifications include: Ph.D. degree at time of appointment, demonstrated potential to start and maintain an active research program through securing external grants, demonstrated potential to publish and otherwise disseminate results of research, and demonstrated potential to perform teaching duties. Applicants should submit a vitae or resume, names and addresses of four references who may be contacted for written evaluations, and a letter of application including a statement of the applicant's teaching and research capabilities and plans. Application materials should be sent to Human Resources, P.O. Box 11127, Lamar University, Beaumont, Texas 77710, Position Number 699697, Attn.: Dr. Joseph Kruger, Earth and Space Sciences Search Committee Chair. Review of the material will begin in February and will continue until the position is filled. Lamar University is a member of the Texas State University System and an AA/EEO Employer.

**FACULTY POSITION**
**GROUNDWATER HYDROLOGY**
**THE UNIVERSITY OF ARIZONA**

The University of Arizona (UA) seeks a faculty member (level open) in Groundwater Hydrology to join the Department of Hydrology and Atmospheric Sciences (HAS) in the UA College of Science. The newly created HAS department (www.has.arizona.edu) merges the previous Department of Atmospheric Sciences with the Department of Hydrology and Water Resources.

The new, tenure-eligible, faculty position will build upon UA's historical strengths in ground- and surface-water hydrology, water quality, and systems analysis, and on its synergistic new programs in Terrestrial Hydrometeorology, climate variability and the coupled human-land atmosphere system.

**Required Background:** The successful candidate will have a strong quantitative understanding of the physics of groundwater flow and transport, as well as the motivation to apply groundwater science towards addressing societal challenges related to water resources (e.g. climate change and environmental contamination), especially in the desert Southwest where groundwater is critically important to our very existence. Candidates with expertise in any area of quantitative groundwater hydrology are encouraged to apply. However, we are particularly interested in applicants who use innovative analytical, quantitative and/or computational tools to investigate the flow of water through saturated and unsaturated geologic media and the interaction of this flow with atmospheric, biological and/or chemical processes.

**Expectations:** The new faculty member will be expected to build a complementary research group to pursue collaborative and ambitious new projects, to strengthen the UA's ability to compete for funding, and to help define scientific priorities for the community. In addition, she/he will be expected to provide innovative and quality teaching, advising and mentoring of students at the graduate and undergraduate levels (including those from underrepresented backgrounds), provide opportunities for student engagement in research, internship and professional training, participate in service and outreach, and promote the UA's goals for broad representation among its students and workforce. In this

**ETH zürich**

## Assistant Professor (Tenure Track) of Structural Geology and Tectonics

→ The Department of Earth Sciences (www.erdw.ethz.ch) at ETH Zurich invites applications for the above-mentioned position.

→ The new assistant professor will be expected to build an outstanding research program investigating aspects of rock or Earth deformation at any temporal and spatial scale from earthquake dynamics to plate motion. Candidates should have a proven research record in the field of tectonics or structural geology. He or she should have an in-depth knowledge of mechanisms and processes of lithospheric deformation across a range of tectonic settings and the ability to conduct geological fieldwork. Ideally, the new assistant professor will complement existing strengths in geosciences at ETH Zurich. The teaching portfolio will be expected to include undergraduate level courses in structural geology, tectonics and field geology; more advanced, graduate level courses will cover additional aspects in his or her areas of expertise.

→ Assistant professorships have been established to promote the careers of younger scientists. ETH Zurich implements a tenure track system equivalent to other top international universities.

→ **Please apply online at www.facultyaffairs.ethz.ch**

→ Applications include a curriculum vitae, a list of publications, a statement of future research and teaching interests, a description of the three most important achievements, and the contact details of three potential referees. The letter of application should be addressed **to the President of ETH Zurich, Prof. Dr. Lino Guzzella. The closing date for applications is 15 February 2017**. ETH Zurich is an equal opportunity and family friendly employer and is responsive to the needs of dual career couples. We specifically encourage women to apply.

regard, we particularly seek individuals who are interested in a) promoting diversity in research, education, and outreach, b) developing innovative approaches to enhancing student engagement, c) participating in outreach and contributing to departmental, college, and university service, d) a variety of collaborative, teaching, and curricular perspectives, and e) expanding collaborations with community and business partners.

**To Apply:** For more information, and to apply for the position, please see the job posting at https://uacareers.com/postings/15210.

### MICHEL T. HALBOUTY '30 VISITING CHAIR IN GEOLOGY AND GEOPHYSICS TEXAS A&M UNIVERSITY

The Department of Geology and Geophysics at Texas A&M University is pleased to announce the Michel T. Halbouty '30 Visiting Chair in Geology and Geophysics. The purpose of Mr. Halbouty's generous gift is to "Promote excellence in the teaching and research of the Department of Geology and Geophysics." We expect to appoint 4 to 5 distinguished scholars to the Visiting Chair over the next few years and provide them the opportunity to visit our campus and interact with department faculty and students for up to twelve months duration. The appointment provides partial salary support and additional funds to cover lodging and travel, as well as proposed engagement activities.

Applications should be submitted by March 20, 2017, to be considered for awards in 2017 and 2018. Interested persons are encouraged to contact faculty members in the Department of Geology and Geophysics (http://geoweb.tamu.edu/). Applications should identify potential faculty proponents, include a CV, a 2-page proposal identifying research, teaching and engagement activities as a Visiting Chair holder, availability for visiting the department in the upcoming academic year, and tabulation of desired funds needed for salary and other expenses.

Texas A&M University is an Affirmative Action/Equal Opportunity Employer committed to excellence through the recruitment and retention of a diverse faculty and student body and compliance with the Americans with Disabilities Act. The University is dedicated to the goal of building a culturally diverse and pluralistic faculty and staff committed to teaching and working in a multicultural environment. We strongly encourage applications from women, underrepresented ethnic groups, veterans, and individuals with disabilities. Texas A&M University also has a policy of being responsive to the needs of dual-career partners (hr.tamu.edu/employment/dual-career.html).

Please send your application materials to F.M. Chester, chair of the Halbouty Visiting Chair Committee (chesterf@tamu.edu). For further information, contact F.M. Chester or other faculty members of the department (http://geoweb.tamu.edu/).

### ASSISTANT PROFESSOR STRUCTURE/TECTONICS WILKES UNIVERSITY

Wilkes University invites applicants for a tenure-track Assistant Professor of Geology in the Environmental Engineering and Earth Sciences Department starting August 2017. The Environmental Engineering and Earth Sciences programs, including Geology, are exclusively undergraduate programs that have a long tradition of personalized learning/teaching experiences with small class sizes, publishable undergraduate research, and hands-on projects throughout the curriculum. The successful applicant would be expected to complement the science and engineering faculty (8 full-time members) and value undergraduate research.

The Department seeks a candidate with expertise in tectonics/structural geology, teaching experience at the undergraduate level in these and related areas, experience mentoring undergraduate level students in research, an ability to work with an interdisciplinary team of faculty and a desire to assist the Department in delivering a modern undergraduate geology major. Teaching and/or research experience that bridges environmental science, energy resources, or a closely related field will be considered favorably. Field-based research and an interest in the North American Appalachian orogenic belt are desirable. The successful candidate is expected to assist in the development of a summer geology field course. Candidates must have earned a doctoral degree at the time of appointment.

Primary teaching duties include courses in tectonics and structural geology, applied geophysics and field methods. We seek a candidate who is able to provide outstanding classroom, laboratory, and in-field instruction and who is amenable to teach courses outside of their specialty area such as hydrogeology, paleontology and energy resources. The successful applicant will be expected to develop a research program that involves undergraduate students and to pursue external research funding.

Wilkes University is an independent, comprehensive university dedicated to academic excellence in the liberal arts, sciences, and selected professional programs. The University has approximately 2300 students at the undergraduate level and over 2,000 full time equivalent students at the graduate and first professional levels. Its institutional focus is on developing strong mentoring relationships with each of its students and contributing vitally to economic development of Northeastern Pennsylvania. The University is located in Wilkes-Barre, Pennsylvania, a revitalized city that is located on the scenic Susquehanna River and is within two and one-half hours driving distance of New York City and Philadelphia.

To apply, visit www.Wilkes.edu and click "Jobs at Wilkes". Please include a cover letter, curriculum vitae, statement of teaching philosophy, and contact information for three references. Review of applications begins February 1, 2017 and will continue until the position is filled. Information on the Department is at http://www.wilkes.edu/academics/colleges/science-and-engineering/environmental-engineering-earth-sciences/.

Wilkes University is constantly seeking to become a more diverse community and to enhance its capacity to value and capitalize on the cultural richness that diversity brings. The University strongly encourages applications from persons with diverse backgrounds.

**John W. (Jack) Hess,** *GSA Foundation President*

# The Value of Mentorship

**Wes Ward and Camera Ford during one-on-one mentoring time at the GSA 2016 Annual Meeting.**

You might have read Foundation updates about GSA's On To the Future initiative since the program's inception in 2013. We are eager to continue telling you about the progress of program alumni, as well as personal experiences of both students and their mentors. GSA is working steadily to increase one-on-one mentoring opportunities, while the Foundation is working steadily to obtain funding in support of this important undertaking.

Wes Ward, current GSAF Trustee, has been engaged in mentoring OTF students for two years. This is no surprise from a two-term chair of GSA's Committee on Women and Minorities (now Diversity) and two-term President of the National Association of Black Geoscientists. Wes's personal passion inspires his participation: "Aside from the satisfaction I get from helping students in the pipeline make their way along (as I was helped long ago), I really am impressed how far GSA's programs to aid underrepresented students have come since I started participating in the middle 1970s. There is an air of dedication from the professionals and a sense of preparedness and eagerness from the students that makes me proud of what the Society is accomplishing. I see more and more that our future is strong with the emergence of these young professionals and I am delighted to engage and equip them as they shape that future."

In 2016 Wes was a mentor to recent Brown graduate Camera Ford. His time was split between talking and listening to her one-on-one and seeking out and introducing her to researchers in her fields of interest or from graduate schools she might wish to attend. Wes said, "I was amazed at the drive she had in asking for information from all those folks. She will do very well in our profession."

From Camera's perspective, being part of On To the Future was incredibly beneficial: "Having a mentor, especially one as wonderful as Wes, made all the difference for me in getting the most out of my GSA meeting experience. I came to the meeting knowing my areas of interest within geoscience, but unsure of where to go next as a recent graduate with wide-ranging career and research aspirations. I really appreciated his willingness to talk to me about his experiences in the geosciences and about my own goals, and to introduce me to people that he knew.

"I have just graduated from Brown University with a bachelor's degree in geology, and at the moment I am completing an internship related to computer programming, web development, and tech entrepreneurship. Moving forward, I want to apply some of these skills towards my interests in geoscience research, policy, and education."

The relationships that unfold and the experiences shared through GSA's expanding mentor opportunities reach far beyond these brief interactions. If you would like to support these programs with funding (**https://www.gsafweb.org/donate/#fund=on-to-the-future-fund**) or your time as a mentor (**www.geosociety.org/mentors**), please find more information at these links, or contact Bill Tortorici at +1-303-357-1007, btortorici@geosociety.org. With every additional person who participates, another student discovers a world of possibilities in the geosciences.

**Camera's tectonics field trip in the Andes in January 2016.**

# 2017 GSA Section Meetings

Aerial overview of the Canyon Lake spillway of south-central Texas. Photo by Larry Walther.

**South-Central Section**
Location: San Antonio, Texas, USA
Dates: 13–14 March
Meeting Chair: Benjamin Surpless, bsurples@trinity.edu
**www.geosociety.org/sc-mtg**

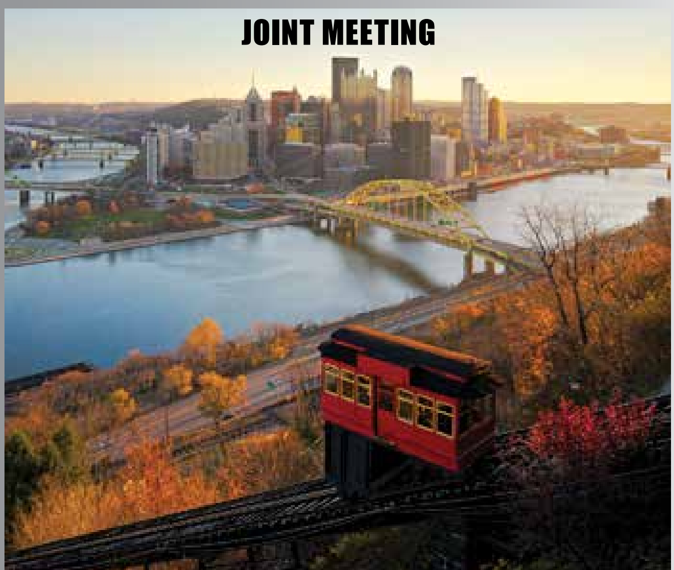


Downtown Pittsburgh from Duquesne Incline.

**Northeastern Section**
(Joint with North-Central Section)
Location: Pittsburgh, Pennsylvania, USA
Dates: 19–21 March
Meeting Chair: Patrick Burkhart, patrick.burkhart@sru.edu
**www.geosociety.org/ne-mtg**

**North-Central Section**
(Joint with Northeastern Section)
Location: Pittsburgh, Pennsylvania, USA
Dates: 19–21 March
Meeting Chair: Timothy G. Fisher, timothy.fisher@utoledo.edu
**www.geosociety.org/nc-mtg**

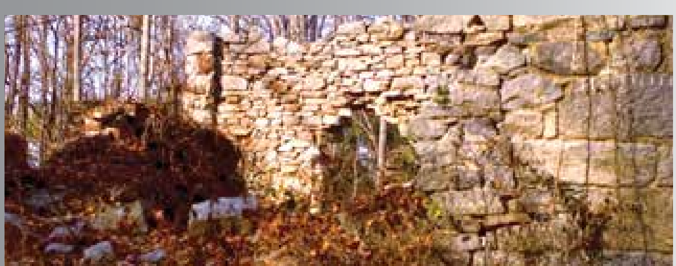

Midlothian Mines. Photo used with permission from Richmond Region Tourism.

**Southeastern Section**
Location: Richmond, Virginia, USA
Dates: 30–31 March
Meeting Co-Chairs: David Spears, david.spears@dmme.virginia.gov; Karen Layou, klayou@reynolds.edu
**www.geosociety.org/se-mtg**

Used with permission from Hawai'i Tourism Authority. Photo by Tor Johnson.

**Cordilleran Section**
Location: Honolulu, Hawaii, USA
Dates: 23–25 May
Meeting Chair: Craig R. Glenn, glenn@soest.hawaii.edu
**www.geosociety.org/cd-mtg**

Three Sisters from the Front Ranges along the Trans Canada Highway near Canmore. Photo by Larry Lane.

**Rocky Mountain Section**
Location: Calgary, Alberta, Canada
Dates: 9–10 June
Meeting Chair: Katherine Boggs, kboggs@mtroyal.ca
**www.geosociety.org/rm-mtg**

**www.geosociety.org/sections**

THE GEOLOGICAL SOCIETY OF AMERICA®

# SCIENCE EDITOR OPENINGS FOR 2018

GSA is soliciting applications and nominations for science co-editors for *Geology*, *GSA Bulletin*, *Geosphere*, and *GSA Today* with four-year terms beginning 1 January 2018. Duties include: ensuring stringent peer review and expeditious processing of manuscripts; making final acceptance or rejection decisions after considering reviewer recommendations; and maintaining excellent content through active solicitation of diverse and definitive manuscripts.

## POSITIONS AVAILABLE

- *GSA Today* ▸ 1 position
- *GSA Bulletin* ▸ 1 position
- *Geosphere* ▸ 1 position
- *Geology* ▸ 1 position

**GSA TODAY** The editor of *GSA Today*, one of the most widely read earth science publications in the world, must have a wide range of interests and expertise along with the ability to identify research topics of both high quality and broad appeal. Prior editing experience and a publication record in a wide range of journals is key.

**GSA BULLETIN** Research interests that would complement those of the continuing editors include, but are not limited to: stratigraphy; geomorphology; geochemistry; tectonics; structural geology; deformation; and paleoclimatology.

**GEOSPHERE** Research interests that would complement those of the continuing editors include, but are not limited to: geochronology; geochemistry; volcanology; petrology; sedimentary geology; remote sensing/GIS; tectonics, structural geology; geosciences education; and dynamic content.

**GEOLOGY** Research interests that would complement those of the continuing editors include, but are not limited to: hard-rock geology; tectonics; geodynamics; geochemistry; tectonophysics; volcanology; marine geology; structural geology; geophysics; and planetary geology.

Note that candidates should not feel they must have expertise in *every* area listed; however, editors will sometimes need to handle papers outside of their main disciplines.

## A SUCCESSFUL EDITOR WILL HAVE

- a broad interest and experience in geosciences, including familiarity with new trends;
- international recognition and familiarity with many geoscientists and their work;
- a progressive attitude and a willingness to take risks and encourage innovation;
- experience with online manuscript systems and the ability to make timely decisions; and
- a sense of perspective and humor.

## INTERESTED?

- Please submit a curriculum vitae and a letter describing why you are suited for the position to Jeanette Hammann, jhammann@geosociety.org.
- To nominate another, submit a nomination letter and the person's written permission and CV.

Editors work out of their current locations at work or at home. The positions are considered voluntary, but GSA provides an annual stipend and funds for office expenses. **DEADLINE** First consideration will be given to nominations or applications received by **15 February 2017**.

**FUTURE OPENINGS** (terms begin January 2019): One position each for *GSA Bulletin, Geosphere, Lithosphere, GSA Books, GSA Today*, and *Environmental and Engineering Geoscience*.